

Cluster extent inference revisited: quantification and localization of brain activity

Jelle J. Goeman* Paweł Górecki[†] Ramin Monajemi* Xu Chen*
Thomas E. Nichols^{‡§} Wouter Weeda[¶]

August 9, 2022

Abstract

Cluster inference based on spatial extent thresholding is the most popular analysis method for finding activated brain areas in neuroimaging. However, the method has several well-known issues. While powerful for finding brain regions with some activation, the method as currently defined does not allow any further quantification or localization of signal. In this paper we repair this gap. We show that cluster-extent inference can be used (1.) to infer the presence of signal in anatomical regions of interest and (2.) to quantify the percentage of active voxels in any cluster or region of interest. These additional inferences come for free, i.e. they do not require any further adjustment of the alpha-level of tests, while retaining full familywise error control. We achieve this extension of the possibilities of cluster inference by an embedding of the method into a closed testing procedure, and solving the graph-theoretic k -separator problem that results from this embedding. The new method can be used in combination with random field theory or permutations. We demonstrate the usefulness of the method in a large-scale application to neuroimaging data from the Neurovault database.

1 Introduction

Functional Magnetic Resonance Imaging (fMRI) studies aim to find brain regions that are activated in response to a mental task. The activity of the brain is measured by the proxy of changes in blood oxygenation levels (BOLD), and researchers look for areas in which these changes are associated with the pattern of the experimental stimulus, e.g. the alternation of task and rest (Ogawa et al., 1992).

From a statistical perspective an fMRI experiment is a huge multiple testing problem. The brain is partitioned into around 200,000 voxels, 3-dimensional equivalents of pixels. For each such voxel a z -score test statistic is calculated that combines the evidence from the BOLD measurements of the experimental subjects. Inference based on these test statistics can be done at the voxel level, resulting in a multiple testing problem with around 200,000 null hypotheses. More commonly, however, fMRI researchers are interested in inference at the level of clusters, sets of connected voxels, with the aim of relating these clusters of activation to certain anatomical areas in the brain (e.g. "listening to sounds is related to increased activation in the left auditory cortex").

*Biomedical Data Sciences, Leiden University Medical Center, Leiden, The Netherlands

[†]Institute of Informatics, Faculty of Mathematics, Informatics and Mechanics, University of Warsaw, Poland

[‡]Big Data Institute, Li Ka Shing Centre for Health Information and Discovery, Nuffield Department of Population Health, University of Oxford, UK

[§]Wellcome Centre for Integrative Neuroimaging, FMRIB, Nuffield Department of Clinical Neurosciences, University of Oxford, UK

[¶]Methodology and Statistics, Psychology, Leiden University, The Netherlands

The standard method for cluster inference is cluster extent thresholding (Friston et al., 1994; Forman et al., 1995; Nichols, 2012). The researcher chooses a z -score cut-off z , finds all voxels with a z -score above z , and identifies supra-threshold connected voxels as clusters. Next, all clusters with an extent (number of voxels) larger than the extent threshold k are declared significant. To control the cluster familywise error rate (FWER), the extent threshold k must be the $(1 - \alpha)$ -quantile of the distribution of the maximal extent of such clusters under the global null hypothesis. It can be determined either analytically, using the assumption that the z -scores come from a Gaussian random field (Worsley et al., 1996; Friston et al., 1994; Eklund et al., 2016), or more robustly by permutations (Hayasaka and Nichols, 2003). Alternatively, the cluster false discovery rate can be controlled, by submitting uncorrected cluster p -values to the Benjamini-Hochberg procedure (Chumbley et al., 2010); other proposals have included controlling the expected number of false positive clusters (Bullmore et al., 1999).

Although the FWER extent threshold k is calculated under the complete null hypothesis, it has been shown that cluster inference has strong control of the FWER (Worsley et al., 1992). This implies that, regardless of the amount of signal present in the data, with probability at least $1 - \alpha$ no cluster null hypothesis is falsely rejected. The cluster null hypothesis is the hypothesis that none of the voxels in the cluster is truly “active”, i.e. associated with the experimental stimulus. The inferential statement that can be made from cluster inference is, therefore, that, with $1 - \alpha$ simultaneous confidence, every significant cluster contains at least one active voxel.

While this cluster-level FWER control is the de facto approach to cluster inference, it has been criticized as insufficient to support the conclusions researchers would typically like to draw from neuroimaging experiments. For example, Woo et al. (2014) argued that, especially at low z thresholds, clusters can become too large and span multiple brain areas, challenging the interpretation of the results. The following three inferential conclusions are often (implicitly or explicitly) drawn from cluster inference result, though they are not supported by the theory.

1. “*A large significant cluster contains a substantial number of active voxels.*” Cluster-level FWER control only supports the statement that at least one voxel in the cluster is confidently active, not that many, or let alone, all voxels are active. This is perhaps one of the most frequent misunderstandings of the current state-of-the-art in cluster inference (Woo et al., 2014).
2. “*A large significant cluster is a more substantial scientific finding than a small significant cluster.*” In fact, the assertion that at least one voxel in a large cluster is active, is a less precise, and therefore weaker finding than the same assertion in a small cluster. This counter-intuitive property is known as the Spatial Specificity Paradox (Woo et al., 2014).
3. “*Substantial overlap between a significant cluster and an anatomical brain area indicates evidence for the presence of activity in that anatomical brain area.*” A significant cluster confidently contains at least one active voxel, but unless that cluster is completely contained in the anatomical area, such activity may lie outside the anatomical brain area (Woo et al., 2014).

Despite its widespread use, cluster-level FWER provides very weak inferences on the nature of non-null signal within a cluster. Still, the three desired conclusions from cluster inference, sketched above, are intuitively quite reasonable. If a cluster exceeds the minimal size k for a significant cluster by a large margin, it is natural to suppose that there is a substantial amount of signal in the cluster, and at least more than in another cluster with an extent just over k . If the large cluster largely overlaps with an anatomical region, it is reasonable to suppose that some of the signal in the cluster must be in the anatomical region.

This paper strengthens cluster inference by presenting an improvement of the method that allows much stronger and more informative conclusions to be drawn, avoiding the problems sketched above. Rather than returning a p -value for each supra-threshold cluster, the new method returns a *true discovery proportion* (TDP) for every region, a simultaneous lower confidence bound for the proportion of truly active voxels in the region

(Genovese and Wasserman, 2006; Goeman and Solari, 2011). By quantifying how widely spread a signal is within a brain region, TDP-based inference avoids the spatial specificity paradox (Rosenblatt et al., 2018). Moreover, TDP can be calculated for any brain region, not just for supra-threshold clusters; this way also the amount of signal in anatomical regions may be assessed.

Analysis of neuroimaging data in terms of TDP rather than p -values was pioneered by Rosenblatt et al. (2018), who proposed the ARI method based on closed testing with the Simes test (Goeman et al., 2019). Other methods for TDP inference suitable for brain imaging include Blanchard et al. (2020); Andreella et al. (2020); Vesely et al. (2021); Blain et al. (2022). The proposed method differs from these methods because it is based on classic extent-based cluster inference, and therefore aligns much more closely with standard practice. Unlike these methods, the new method will always yield $\text{TDP} > 0$ for any cluster that is significant according to classic cluster-based inference. In fact, there is no power loss when switching from classic cluster-based inference to the method proposed in this paper; the new method is a uniform improvement (in the sense of Goeman et al., 2021) of classic cluster-based inference. Moreover, the new method retains strict FWER control over all reported findings: with probability at least $1 - \alpha$ no reported TDP is greater than the proportion of truly active voxels in the corresponding region.

We construct the improvement of cluster inference by remarking that cluster inference is a special case of a true discovery guarantee method, as defined by Goeman et al. (2021). Viewed in this way, cluster inference is not admissible, but can be uniformly improved by embedding it into a closed testing procedure, which we will construct. The local test of this procedure rejects the null hypothesis of no activity in a subset of the brain whenever that subset contains a connected subset of size at least k for which all voxel z -scores are above z .

A major challenge of constructing closed testing procedures is, as always, computational. We will show that calculating TDP for a brain region amounts to solving an instance of a graph-theoretic k -separator problem (Ben-Ameur et al., 2015). We propose two novel and fast algorithms to solve the k -separator problem in the lattice graph induced by brain connectivity, in order to find shortcuts for the closed testing procedure.

To illustrate the performance of the method we will apply the novel lower bound on 818 data sets from the Neurovault database (Gorgolewski et al., 2015). We will first illustrate the intended workflow of the new method using an n -back working memory data set (Barch et al., 2013), which we will introduce in the next section as a motivating example.

2 Motivating example

We will first illustrate and preview the new method with a concrete motivating example. The Human Connectome Project (HCP; Van Essen et al., 2013) consists of neuroimaging data of over 5000 subjects performing multiple cognitive tasks. In our example we will use fMRI data obtained from 80 unrelated individuals, each performing an n -back working memory task (Barch et al., 2013). During this task participants are sequentially shown a series of letters (e.g. “E”, “D”, “Z”, “X”, “M”). After the sequence is shown participants are asked to recall letters from a specific position in the sequence. For example, in the 0-back condition this is the last letter shown (“M”), in the 2-back condition this is the letter in second-to-last position (“Z”). In n -back tasks, higher values of n are theoretically associated with larger memory load for the participants. We focused on the 2-back versus 0-back contrast, for which the null hypothesis of interest per voxel was that the BOLD signal was identically distributed between the 2-back and 0-back conditions. For the calculation of per-voxel test statistics, we followed a standard processing pipeline (Glasser et al., 2013) using FSL (Woolrich et al., 2001), a popular software package for cluster extent inference. This is a two-stage analysis, in which the 2-back versus 0-back contrast is first analyzed for each subject separately and the results are subsequently aggregated across subjects into a group-level z -statistic for each of the 257,659 voxels in the brain, using standard methods described by Beckmann et al. (2003). Each of these z -statistics is standard normal under their respective per-voxel null hypothesis.

Before seeing the data, a cluster-forming threshold of $z = 3.1$ was chosen. Clusters were formed by all connected neighboring supra-threshold voxels. Using standard theory, which we will revisit in Section 3, a permutation-based extent threshold of 72 was found, indicating that all clusters consisting of more than 72 voxels are significant. This led to 6 significant clusters and several non-significant clusters. The details of the significant clusters are shown in Figure 1 and Table 1.

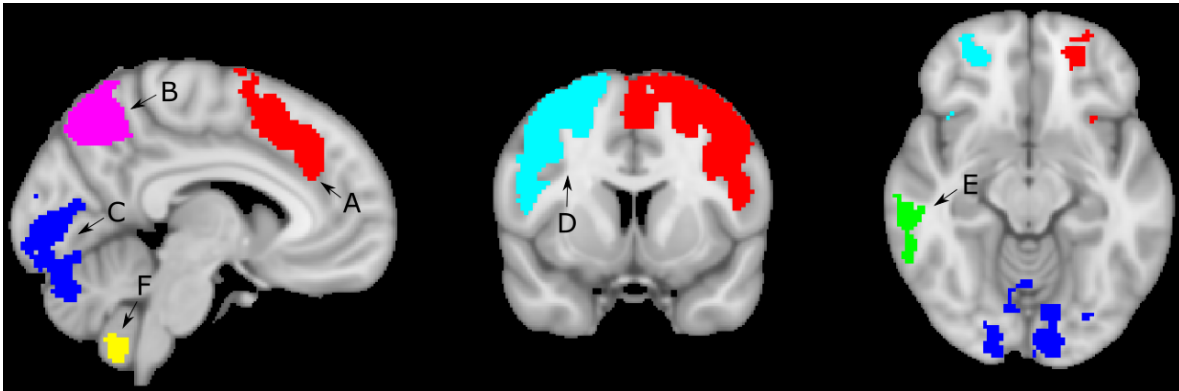


Figure 1: Task-related brain activation for the 2-back versus 0-back contrast across all subjects. Six significant clusters A, B, C, D, E, F are displayed using different colors.

Table 1: Task-related brain activation for the 2-back versus 0-back contrast across all subjects. Columns show the size, p -value, maximum z -statistic, and coordinates of the maximum for all clusters.

Cluster	Size	p -value	$\max(z)$	X	Y	Z
A	8870	< 0.001	8.87	44	72	60
B	8526	< 0.001	9.51	19	42	61
C	7956	< 0.001	9.20	63	33	20
D	6652	< 0.001	9.73	31	67	64
E	350	0.004	5.18	15	46	28
F	100	0.027	6.56	49	35	10

With classic cluster inference, the analysis ends here. The researchers may claim that some signal is present in each significant cluster, but the amount of signal is undetermined. This is especially tantalizing for the biggest cluster A, that visually consists of several sub-regions. No statement can be made about the presence of signal in these sub-clusters. Cluster C overlaps for a large part with the cerebellum, but since it is not fully contained in the cerebellum, the researcher may not confidently claim the presence of signal here from the overlap with Cluster C. In contrast, Cluster F, which is relatively small and would not attract the most attention in the publication, does substantiate a claim about the presence of signal in the cerebellum since it is completely contained in it. Paradoxically, Cluster F is the most precise finding, since it localizes the presence of signal to a precision of no more than 100 voxels.

The theory developed in this paper will allow much more informative statements to be made about clusters A, to F.

1. We calculate a true discovery proportion (TDP) per cluster, a lower bound to the number of truly active voxels. Clusters A, B, C, D, E, F get TDPs of 37%, 40%, 33%, 37%, 19% and 10%, respectively. This

indicates that clusters A to D are the main findings of the experiment, but shows that the localization of the signal is only moderately precise.

2. We also find TDPs for any other (anatomical) brain regions of interest. We find, for example, significant evidence of signal in cerebellum, mostly from the overlap with cluster C, though with a small TDP of 5.8%.

The TDP values we find are guaranteed to be consistent with the cluster p -values in the sense that $p \leq 0.05$ if and only if TDP is positive. Compared to the p -values, the TDP is more informative since it quantifies the pervasiveness of the signal within the cluster. The full analysis results are given in Section 9.

3 Classic cluster inference

We start by briefly revisiting classic cluster inference. We will follow the notational conventions used in Goeman et al. (2021) that, except for the probability distribution P , all capitals are sets and all lower case variables are scalars or vectors. Random variables are in boldface.

3.1 Voxels and clusters

The brain is partitioned into hundreds of thousands of voxels, forming a rectangular grid. With suitable coordinates each voxel can be identified as a point in \mathbb{Z}^d . We will usually think of $d = 3$, but we will write our theory for general $d \geq 1$. The brain $B \subset \mathbb{Z}^d$ is an irregularly shaped, finite collection of voxels. It is not always the entire brain that is of interest to the researcher, and a mask $M \subseteq B$ is chosen, before seeing the data, limiting all inference to voxels in M .

We define a neighbor relationship between voxels, saying that voxels $v, w \in \mathbb{Z}^d$ are neighbors if $v - w \in \{-1, 0, 1\}^d$. This neighborhood definition is known as 26-connectivity in neuroimaging since it gives each voxel 27 neighbors (26 plus itself) if $d = 3$.

The voxels and the neighbor relation together induce an undirected graph when the voxels are seen as nodes and the neighbor relationships as edges. We call a voxel set $V \subseteq \mathbb{Z}^d$ a *cluster* if its induced graph is connected, i.e. if we can traverse from every voxel in V to every other voxel in V by passing from neighbor to neighbor. We call voxel sets V and W *disconnected* if no voxel of V is a neighbor of a voxel of W .

3.2 Voxel null hypotheses and z -scores

Let Ω be our statistical model and $P \in \Omega$ the unknown probability distribution of the data. For each voxel $v \in M$ we define a voxel-wise null hypothesis $H_v \subseteq \Omega$ stating that the voxel v is not active, i.e. that the BOLD signal for that voxel is not related to the experimental stimulus. Note that in general a hypothesis H is true if and only if $P \in H$.

An fMRI experiment typically involves several subjects that are measured for a prolonged time period, leading to a huge data set with a BOLD observation per subject per voxel per time point. In the first steps of the analysis, for every $v \in B$, these data are aggregated to a single z -score \mathbf{z}_v per voxel that represents the evidence against the voxel null hypothesis from the experiment. We refer to Lindquist (2008) for a description of the analysis steps involved. In this paper we assume that the first steps of the analysis have already been done, and we start from z -scores $(\mathbf{z}_v)_{v \in B}$. The z -score \mathbf{z}_v is expected to be small in absolute value if H_v is true and large if H_v is false.

3.3 Voxel set null hypotheses and the cluster extent threshold

Researchers are usually not particularly interested in individual voxels, since these are considered too small to represent relevant brain processes. Instead, researchers look at clusters of neighboring voxels. For every voxel set $V \subseteq M$, we define the voxel set null hypothesis as $H_V = \bigcap_{v \in V} H_v$. This hypothesis states that all of the voxelwise null hypotheses for voxels in V are true, i.e. that none of the voxels in V are active. The hypothesis $H_\emptyset = \Omega$ is always true.

Cluster inference uses the voxel z -scores to make inference at the cluster level. First, before seeing the data the researcher selects a z -score cut-off z . Next, the researcher finds the set of all supra-threshold voxels in the mask, $M \cap \mathbf{Z}$, where

$$\mathbf{Z} = \{v \in B: \mathbf{z}_v > z\} \quad (1)$$

is the collection of all supra-threshold voxels. Equation (1) uses one-sided tests. Two-sided tests can be done either using $|\mathbf{z}_v| > z$ in (1) or by repeating the analysis twice: once with \mathbf{z}_v and once with $-\mathbf{z}_v$, using half the α -level.

The supra-threshold voxel set $\mathbf{Z} \cap M$ is not in general a cluster, but it is always a union of clusters. We can uniquely write $\mathbf{Z} \cap M = \mathbf{C}_1 \cup \dots \cup \mathbf{C}_n$, where $\mathbf{C}_1, \dots, \mathbf{C}_n$ are disconnected clusters. Cluster inference now claims the presence of signal in every \mathbf{C}_i for which $|\mathbf{C}_i| > k_M$, where $|\cdot|$ is the cardinality of a set, and k_M is the cluster extent threshold calculated for mask M . The cluster extent threshold is defined as the $(1 - \alpha)$ -quantile of the maximum size of a supra-threshold cluster under the global null. Formally, the size of the largest supra-threshold voxel is $\chi_{M \cap \mathbf{Z}}$, where

$$\chi_V = \max\{|\mathbf{C}|: \mathbf{C} \subseteq V \text{ is a cluster}\}.$$

This maximum is always defined since the empty set is a cluster. The cluster extent threshold k_M therefore has the property that, for every $P \in H_M$,

$$P(\chi_{M \cap \mathbf{Z}} > k_M) \leq \alpha. \quad (2)$$

We remark that k_M is allowed to be random, as it would be e.g. in permutation approaches. We also remark that we deviate slightly from the usual definition of k_M , which uses \geq in the first inequality in (2).

To achieve (2) various assumptions have been proposed. Friston et al. (1994) assumes that $(z_v)_{v \in M}$ follows a stationary Gaussian random field on M , and that each $H_v, v \in B$, is the hypothesis that z_v has zero mean. In this case, k_M can be approximated using the expected Euler characteristic of the field, and (2) holds as long as z is large enough and the field is sufficiently smooth (Worsley et al., 1996; Eklund et al., 2016). Alternatively, a k_M achieving (2) may be calculated from other assumptions, e.g. using permutations (Hayasaka and Nichols, 2003), t -fields, χ^2 -fields, or F -fields (Worsley et al., 1996). In the rest of the paper we will not use any specific set of distributional assumptions. We will simply assume k_M can be calculated for every $M \subseteq B$ such that (2) holds.

Larger masks allow larger supra-threshold clusters, and therefore larger cluster extent thresholds. We will assume that if $M \subseteq N$, then,

$$k_M \leq k_N. \quad (3)$$

This relationship is natural since $\chi_{M \cap \mathbf{Z}} \leq \chi_{N \cap \mathbf{Z}}$, surely. It can be verified that (3) holds for all ways of calculating k_M described above, provided in Gaussian random fields the smoothness is estimated once based on the largest mask.

4 Closed testing for cluster inference

Having described classic cluster inference we can now construct its embedding into a closed testing procedure. We will use the theory of Goeman et al. (2021), who provide a general method to construct a closed testing

procedure from an existing multiple testing procedure. The proofs of all Lemmas and Theorems are in the Supplemental Information, Section A.

4.1 Local test

A closed testing procedure is built from local tests, which are hypothesis tests for a voxel set null hypothesis H_V . We will define such a local test for every voxel set $V \subseteq M$. For $V = \emptyset$ we may take $k_V = 0$ without loss of generality.

Following Goeman et al. (2021) we note that in the discussion in the previous section the mask $M \subseteq B$ was arbitrary, and that the conclusions of that section hold for any fixed $M \subseteq B$. Following Goeman et al. (2021), Theorem 2, we define as the local test for H_V the test that rejects when cluster inference with mask $M = V$ rejects at least one voxel set null hypothesis. This test rejects when $\phi_V = 1$, where

$$\phi_V = \mathbb{1}\{\chi_{V \cap \mathbf{Z}} > k_V\}. \quad (4)$$

This is a valid local test due to the assumption that (2) holds for every $M \subseteq B$, and therefore for $M = V$: we have for every $P \in H_V$ that $P(\phi_V = 1) \leq \alpha$. If $V = \emptyset$, then $\phi_V = 0$, so the test never rejects. We will use the local test (4) for every $V \subseteq M$ as the building block for the new closed testing procedure.

4.2 Effective local test

The local test ϕ_V is a valid hypothesis test for the presence of signal in V if the researcher restricted attention to V before seeing the data. If the researcher chooses $V \subseteq M$ after seeing the data, a multiple testing correction needs to be performed over all $2^{|M|}$ hypothesis choices $(H_V)_{V \subseteq M}$. This is what closed testing does.

Marcus et al. (1976) proved that such correction for multiple testing can be achieved by the effective local test, defined for any local test as

$$\psi_V = \min\{\phi_W : V \subseteq W \subseteq M\}.$$

The effective local test controls voxel set-level FWER over all $(H_V)_{V \subseteq M}$, having the property that for every $P \in \Omega$,

$$P(\psi_V = 0 \text{ for all } V \subseteq M \text{ with } P \in H_V) \geq 1 - \alpha. \quad (5)$$

Remembering that $P \in H_V$ if and only if H_V is true, we see that with probability at least $1 - \alpha$ no true voxel set null hypothesis is rejected even when ψ_V is applied on all $V \subseteq M$.

4.3 Shortcut

However, ψ_V is difficult to calculate, since it involves calculating ϕ_W , and therefore k_W , for exponentially many $V \subseteq W \subseteq M$. We propose to approximate ψ_V for every $V \subseteq M$ by an alternative test that is easier to compute:

$$\underline{\psi}_V = \mathbb{1}\{\chi_{V \cap \mathbf{Z}} > k_M\}.$$

For every $V \subseteq M$, the test $\underline{\psi}_V$ rejects at most as often as ψ_V , as Lemma 1 states.

Lemma 1. *For every $V \subseteq M$, we have $\underline{\psi}_V \leq \psi_V$.*

The alternative test $\underline{\psi}_V$ is a shortcut for the effective local test ψ_V : it sacrifices some power for ease of computation. By Lemma 1, $\underline{\psi}_V$ retains the error guarantees of ψ_V . Combining the lemma with (5) we obtain voxel set-level FWER for $\underline{\psi}_V$. For every $P \in \Omega$,

$$P(\underline{\psi}_V = 0 \text{ for all } V \subseteq M \text{ with } P \in H_V) \geq 1 - \alpha.$$

We can check that the test ψ_V reproduces all the results of classic cluster inference. Classic cluster inference rejects all clusters $\mathbf{C} \subseteq M \cap \mathbf{Z}$ with $|\mathbf{C}| > k_M$. For such \mathbf{C} , we have $\chi_{\mathbf{C} \cap \mathbf{Z}} = \chi_{\mathbf{C}} = |\mathbf{C}| > k_M$, so that $\underline{\psi}_{\mathbf{C}} = 1$.

However, $\underline{\psi}_V$ allows useful additional conclusions that are not endorsed by classic cluster inference. If $A \subseteq B$ is an anatomical region of interest, we may reject H_A and claim the presence of activity in A if $\chi_{A \cap \mathbf{Z}} > k_M$, that is when there are at least k_M connected supra-threshold voxels within A . This provides a partial solution to the desired inference problem 3 in the introduction to this paper, since it defines precisely how large a ‘substantial overlap’ between a significant cluster and an anatomical region must be to allow a claim of activity in the region: the overlap must contain a connected area of size at least k_M . Note that the region of interest A does not have to be chosen before seeing the data for such inference to be valid, since FWER control is over all $V \subseteq M$.

4.4 True discovery proportions from closed testing

The major gain of the closed testing formulation is not in voxel-set level FWER control, but in simultaneous TDP lower bounds for every cluster. We will use the methods of Genovese and Wasserman (2006) and Goeman and Solari (2011).

Let $A_P = \{v \in B : P \notin H_v\}$ be the set of all truly active voxels in the brain. For voxel set $V \subseteq B$ the number of truly active voxels in V is

$$a_P(V) = |V \cap A_P|.$$

If the researcher would claim that voxel set V is active, the researcher would be right about $a_P(V)$ voxels, and wrong about $|V| - a_P(V)$ of them. We call

$$\pi_P(V) = \frac{a_P(V)}{|V|},$$

or 0 if $V = \emptyset$, the true discovery proportion (TDP) of set V . This is our target of inference. We will infer on $\pi_P(V)$ through $a_P(V)$, which is easier to work with.

Goeman and Solari (2011) proved that, for any closed testing procedure with effective local tests $(\psi_V)_{V \subseteq M}$, random variables defined, for all $V \subseteq M$, as

$$\mathbf{a}(V) = \min\{|V \setminus W| : W \subseteq V, \psi_W = 0\}, \quad (6)$$

have the property that, for all $P \in \Omega$,

$$P(\mathbf{a}(V) \leq a_P(V) \text{ for all } V \subseteq M) \geq 1 - \alpha. \quad (7)$$

A lower bound for the TDP follows immediately: $\pi(V) = \mathbf{a}(V)/|V|$, or 0 if $V = \emptyset$, is a simultaneous lower bound for the TDP all $V \subseteq M$. By (7), for all $P \in \Omega$, we have

$$P(\pi(V) \leq \pi_P(V) \text{ for all } V \subseteq M) \geq 1 - \alpha.$$

As argued by Goeman and Solari (2011), the lower bound $\mathbf{a}(V)$, and its companion $\pi(V)$ provide much stronger statements than the effective local test. Where ψ_V only gives confidence whether or not there is signal present in V , $\mathbf{a}(V)$ gives confidence for the amount of signal. There is no information lost in reporting the TDP $\mathbf{a}(V)$ rather than rejection or non-rejection ψ_V , since $\mathbf{a}(V) \geq \psi_V$, as follows immediately from the definition. The simultaneity of (7) implies familywise error control over all $V \subseteq M$ considered or reported: with probability at least $1 - \alpha$ no reported $\mathbf{a}(V)$, $V \subseteq M$, overestimates the number of truly active voxels $a_P(V)$ in V , even if V was chosen after seeing the data.

4.5 Applying the shortcut

Since $\mathbf{a}(V)$ involves the expression ψ_V , which is difficult to calculate, we use the shortcut $\underline{\psi}_V$ to get a partial shortcut for $\mathbf{a}(V)$. We write

$$\check{\mathbf{a}}(V) = \min\{|V \setminus W|: W \subseteq V, \underline{\psi}_W = 0\}.$$

By Lemma 1, $\check{\mathbf{a}}(V) \leq \mathbf{a}(V)$, so $\check{\mathbf{a}}(V)$ inherits the property (7). Moreover, $\check{\mathbf{a}}(V)$ can be rewritten in a relatively simple form. The formulation of $\check{\mathbf{a}}(V)$ and its property are our first main result. We formulate it as a theorem.

Theorem 1. *Let*

$$\check{\mathbf{a}}(V) = s_{k_M}(V \cap \mathbf{Z}), \quad (8)$$

where $s_k(V) = \min\{|R|: \chi_{V \setminus R} \leq k\}$. Then, for all $P \in \Omega$,

$$P(\check{\mathbf{a}}(V) \leq \alpha_P(V) \text{ for all } V \subseteq M) \geq 1 - \alpha. \quad (9)$$

Although $\check{\mathbf{a}}(V)$ may yield smaller TDP than $\mathbf{a}(V)$, the resulting TDP lower bounds are still at least as powerful as the statements of classic cluster inference, as the next theorem asserts: all clusters found by classic cluster inference have a strictly positive TDP bound.

Theorem 2. *If $\mathbf{C} \subseteq (\mathbf{Z} \cap M)$, with $|\mathbf{C}| > k_M$, is a cluster, then $\check{\mathbf{a}}(\mathbf{C}) > 0$.*

5 Calculating true discovery proportions

The shortcut (8) reduces a computation time of $\mathbf{a}(V)$ that is exponential in $|M|$ to a computation time for $\check{\mathbf{a}}(V)$ that is exponential in $|V|$. This is still prohibitive for most regions V . In this section we discuss algorithms for $\check{\mathbf{a}}(V)$. We show that this calculation is equivalent to solving a problem known as the k -separator problem in graph theory. For the specific case of that problem in the voxel graph with 26-connectivity, we obtain a lower bound to $\check{\mathbf{a}}(V)$ that has computation time $O(|V|^{1+1/d})$, and a fast heuristic algorithm, coupled with simulated annealing, that approaches $\check{\mathbf{a}}(V)$ from above. Both the lower bound and the simulated annealing algorithm rely on a duality between our k -separator problem and tiling problem on a slightly larger object, which we will derive and explain.

5.1 The k -separator problem

From Theorem 1 we see that we have efficient computation of $\check{\mathbf{a}}(V)$ whenever we can efficiently compute $s_k(V)$, for $V \subseteq \mathbf{Z}$. The value of $s_k(V)$ is the minimum number of voxels that must be removed from V in order that the remainder falls apart into disconnected components of size k . The quantity $s_k(V)$ can be defined for any graph, and is known in graph theory literature as the k -separator problem (Ben-Ameur et al., 2015). The k -separator problem is NP-hard, even for small fixed values of k . For example, with $k = 1$ we have a classic vertex cover problem (NP-hard), while for $k = 2$ the problem is equivalent to the computation of dissociation number which is NP-complete for a class of bipartite graphs (Yannakakis, 1981). Ben-Ameur et al. (2015) proposed polynomial time solutions to several constrained variants of the k -separator problem; however, none of them is applicable in our case. In the next few sections we present novel solutions tailored to the specific type of graph induced by the neuroimaging context.

5.2 Preliminaries

Any voxel set V can always be written as a union of disconnected clusters. The next lemma says that it is sufficient to calculate s_k for these clusters.

Lemma 2. *If $V = C_1 \cup \dots \cup C_n$, where C_1, \dots, C_n are disconnected clusters, then*

$$s_k(V) = \sum_{i=1}^n s_k(C_i).$$

Without loss of generality, therefore, we can focus on calculating $s_k(V)$ only for $V \subseteq B$ that are clusters. However, the results in the remainder of this section are for general voxel sets V .

5.3 Positive neighbors

For our solutions to the k -separator problem we will exploit a duality between k -separating V and tiling a somewhat larger object. To construct this duality we first need to introduce to \mathbb{Z}^d the directed relationship of being ‘positive neighbors’.

We say that $w \in \mathbb{Z}^d$ is a *positive neighbor* of $v \in \mathbb{Z}^d$ if $w - v \in \{0, 1\}^d$. We write

$$\{v\}^+ = \{v + e : e \in \{0, 1\}^d\}$$

for the voxel set of all positive neighbors of v . If $w \in \{v\}^+$ we call v a *negative neighbor* of w , since $v - w \in \{-1, 0\}^d$. Note that the positive and negative neighbors do not partition the neighbors. For example, if $d = 2$, $w = (-1, 1)$, though a neighbor of $v = (0, 0)$, is neither its positive or its negative neighbor. Moreover, every v is always both a positive and a negative neighbor of itself.

The concept of the positive neighbors allows the definition of three useful derived voxel sets from every finite voxel set $V \subset \mathbb{Z}^d$. We define the *cover* V^+ of V as

$$V^+ = \{v + e : v \in V, e \in \{0, 1\}^d\} = \bigcup_{v \in V} \{v\}^+$$

the set of all voxels in V and their positive neighbors. The *interior* V^- of V is

$$V^- = \{v \in V : v + e \in V \text{ for all } e \in \{0, 1\}^d\}.$$

the set of all $v \in V$ that only have positive neighbors in V . Finally, the *shave* of V is $V^0 = V \setminus V^-$. This is the ‘positive edge’ of V , the set of voxels in V that have at least one positive neighbor outside V . These three derived voxel sets will allow us to rewrite the k -separator problem into a tiling problem.

5.4 Tiling

To calculate $s_k(V)$ we are interested in k -separators, defined as voxel sets $R \subseteq V$ with the property that $\chi_{V \setminus R} \leq k$. The value of $s_k(V)$ is the minimum $|R|$ over all k -separators. In this section we will show that minimizing $|R|$ over all k -separators is equivalent to minimizing a function $t_k(T_1, \dots, T_n)$ over all tilings T_1, \dots, T_n of V^+ . The latter will turn out to be an easier problem formulation to work with.

Define a *tiling* of V^+ as a collection of pairwise disjoint voxel sets T_1, \dots, T_n , called *tiles*, such that $\bigcup_{i=1}^n T_i = V^+$. Note that every two distinct tiles from a tiling are disjoint as sets but their voxels may induce a connected graph. Given a tiling T_1, \dots, T_n of V^+ , we will be interested in the function

$$t_k(T_1, \dots, T_n) = \sum_{i=1}^n |T_i^0 \cap V| + \sum_{i=1}^n (|T_i^- \cap V| - k)_+, \quad (10)$$

where $(\cdot)_+$ is the positive part function. This function is the link between tilings and k -separators, as the following two lemmas state.

Lemma 3. For every tiling T_1, \dots, T_n of V^+ there exists a k -separator R of V such that

$$|R| = t_k(T_1, \dots, T_n).$$

Lemma 4. For every k -separator R of V there exists a tiling T_1, \dots, T_n of V^+ such that T_1, \dots, T_n are clusters, and

$$|R| \geq t_k(T_1, \dots, T_n).$$

To get some intuition why these lemmas are true, it is helpful to consider a property of neighbors and positive neighbors proven as Lemma 9 in the Supplemental Information, Section A: two voxels are neighbors if and only if they have a common positive neighbor. It follows that voxel sets V and W are disconnected if and only if V^+ and W^+ are disjoint. It is this connection between disconnectedness of sets and simple disjointness of slightly larger sets that is exploited in Lemmas 3 and 4. Loosely, if R cuts V as $V \setminus R = C_1 \cup \dots \cup C_n$, with C_1, \dots, C_n pairwise disconnected, then $C_1^+, \dots, C_n^+ \subseteq V^+$ are pairwise disjoint tiles. Vice versa if $T_1, \dots, T_n \subseteq V^+$ are pairwise disjoint tiles, then their interiors $T_1^-, \dots, T_n^- \subseteq V$ are pairwise disconnected; if these interiors are of size at most k , then $R = (T_1^0 \cup \dots \cup T_n^0) \cap V$ separates V . We illustrate the link between k -separator and tiling with an example in Figure 2.

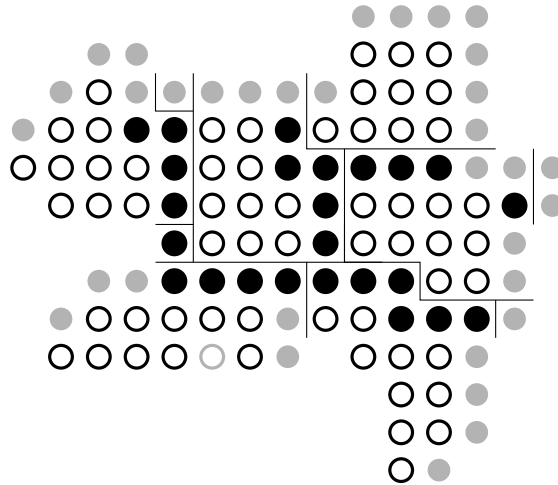


Figure 2: Illustration of a k -separator and a corresponding tiling, with $d = 2$ and $k = 10$. The voxel set V comprises of all black voxels (open and filled). The set V^+ comprises of V and all the gray voxels (open and closed). The k -separator R is the set of all filled black voxels. The corresponding tiling is indicated by the lines. All filled voxels are part of the shave T^0 for their respective tile T ; open voxels are part of the interior T^- .

Combining Lemmas 3 and 4, it follows that minimizing $|R|$ over all k -separators is equivalent to minimizing $t_k(T_1, \dots, T_n)$ over all tilings. We formulate this result as a theorem.

Theorem 3. We have

$$s_k(V) = \min\{t_k(T_1, \dots, T_n) : T_1, \dots, T_n \text{ is a tiling of } V^+\}.$$

The minimum is attained for a tiling for which T_1, \dots, T_n are all clusters.

Theorem 3 rewrites the k -separator problem but does not simplify it. There is no obvious way to minimize $t_k(T_1, \dots, T_n)$ in polynomial time. However, we will exploit this theorem in the next three sections to construct a lower bound to $s_k(V)$, and a heuristic approximation to it.

5.5 A lower bound

First, we construct a lower bound to $s_k(V)$. Replacing $s_k(V)$ by its lower bound in Theorem 1 retains the TDP guarantee implied by that theorem. As a consequence, the lower bound will be a shortcut to the closed testing procedure: it retains the guarantee on the TDP, but sacrifices some inferential power for computational reasons. We will derive this shortcut in two stages. First, in this section, we will calculate a shortcut with $O(|V|)$ time complexity. Next, in Section 5.6, we will construct a more powerful shortcut in $O(|V|^{1+1/d})$ time.

The rationale behind the shortcut is that to minimize the expression (10) we should favor tiles T with $|T^- \cap V| \leq k$, since for such tiles the second term of (10) disappears. For such tiles, minimizing t amounts to finding tiles T with as small as possible edge ratio $|T^0|/|T|$. However, if $|T^-| \leq k$, the edge ratio is bounded from below by the most efficient such ratio possible. This optimal edge ratio r_k can be used to bound $s_k(V)$. We formulate this result as Theorem 4.

Theorem 4.

$$s_k(V) \geq r_k \cdot |V^+| - |V^+ \setminus V|,$$

where

$$r_k = \min\{|V^0|/|V| : \emptyset \neq V \subset \mathbb{Z}^d, |V^-| \leq k\}. \quad (11)$$

Define $\underline{s}_k(V) = r_k \cdot |V^+| - |V^+ \setminus V|$. How can we interpret this lower bound? We see that $\underline{s}_k(V)$ is large if its size $|V|$ is large relative to the size $|V^+|$ of its cover. It takes large values therefore for large and compact V , and small values for smaller or irregular sets V . The calculation of r_k is given in Lemma 5. We plot r_k for $k = 1, \dots, 100$ and $d = 2, 3, 4$ in figure 3.

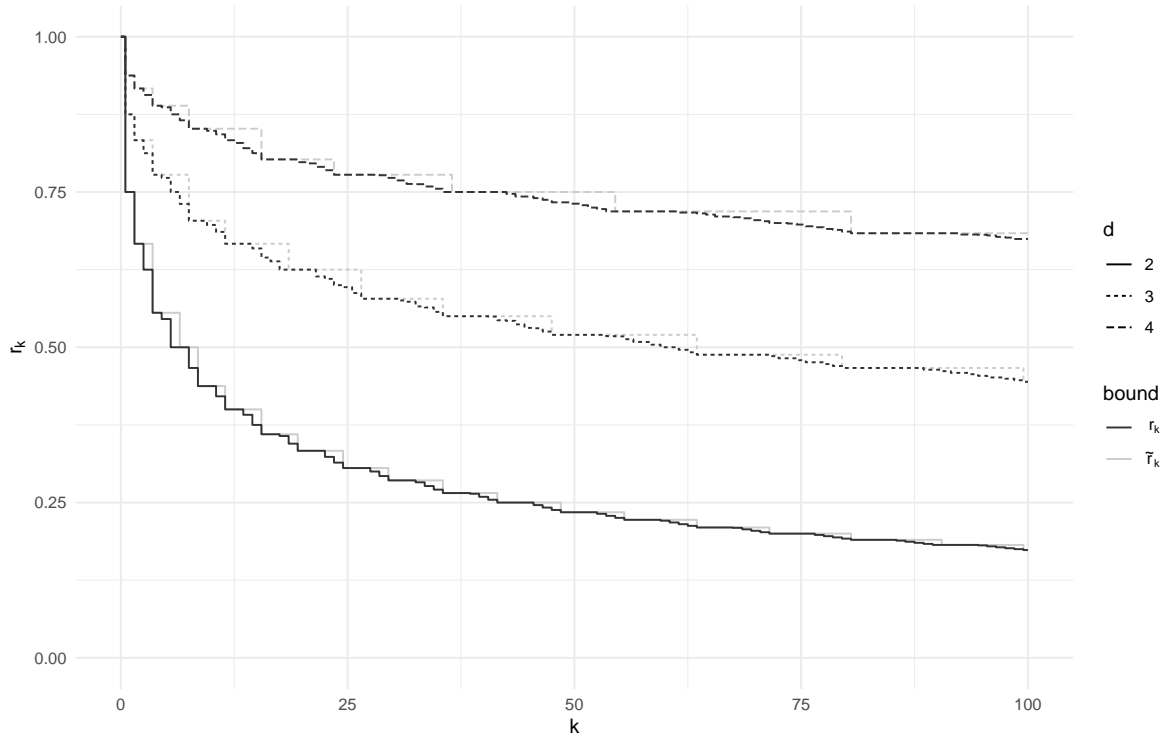


Figure 3: The thresholds r_k and \tilde{r}_k , defined in Theorem 4 and Lemma 8, respectively, as a function of the extent threshold k for dimensions $d = 2, 3, 4$.

Lemma 5. *If $k = 0$, we have $r_k = 1$. If $k > 0$, we have*

$$r_k = \min_{1 \leq j \leq k} \frac{f_{d,j} - j}{f_{d,j}},$$

where $f_{d,k} = 0$ if $d = 0$ or $k = 0$, and, for $d > 1$, we have recursively

$$f_{d,k} = b_{d,k}^+ + f_{d-1,k-b_{d,k}}.$$

Here,

$$b_{d,k} = (\lfloor k^{1/d} \rfloor)^{d-l_{d,k}} (\lfloor k^{1/d} \rfloor + 1)^{l_{d,k}},$$

and

$$b_{d,k}^+ = (\lfloor k^{1/d} \rfloor + 1)^{d-l_{d,k}} (\lfloor k^{1/d} \rfloor + 2)^{l_{d,k}},$$

where

$$l_{d,k} = \left\lfloor \frac{\log(k) - d \log(\lfloor k^{1/d} \rfloor)}{\log(\lfloor k^{1/d} \rfloor + 1) - \log(\lfloor k^{1/d} \rfloor)} \right\rfloor.$$

In the example object of Figure 2, we find from Lemma 5 that with $d = 2$ and $k = 10$ we have $r_k = 7/16$. With $|V| = 84$ and $|V^+| = 118$, we get $\underline{s}_k(V) = 17.6$, so $s_k(V) \geq 18$.

5.6 Pruning

Irregularly shaped objects V have low $\underline{s}_k(V)$. It can therefore pay to prune V to $V' \subseteq V$ in order to bound $s_k(V)$ from below by $\underline{s}_k(V') \leq s_k(V') \leq s_k(V)$. We will use this to get an improved bound on $s_k(V)$.

Suitable choices are $V' = (V^-)^+$, $V'' = (((V^-)^-)^+)^+$, etc., which prune away increasingly broad extremities of V . We illustrate V' in Figure 4. In this example we have $|V'| = 78$, $|(V')^+| = 106$, and we find $\underline{s}_k(V') = 18.4$, so $s_k(V) \geq 19$. Further pruning to V'' leads to $|V''| = 69$ and $|(V'')^+| = 92$ for $\underline{s}_k(V'') = 17.3$ (see figures in the Supplemental Information, Section C). Further pruning does not lead to better bounds. In any case, as Lemma 6 states, pruning more than $|V|^{1/d}$ times is never necessary.

Lemma 6. *If $i \geq \lfloor |V|^{1/d} \rfloor$, then $V^{(i)} = \emptyset$.*

Taking pruning into account, and using that $s_k(V) > 0$ if $|V| > k$, we define the improved bound

$$\check{s}_k(V) = \mathbb{1}\{\chi_V > k\} \vee \max \left\{ \left[\underline{s}_k(V^{(i)}) \right] : i = 0, 1, \dots, |V|^{1/d} \right\},$$

where $V^{(i)}$ is obtained from V by performing the $(\cdot)^-$ operation i times, followed by the $(\cdot)^+$ operation i times.

Taking everything together, the proposed procedure and its TDP guarantee property are summarized in the following theorem, which proves that the lower bound is a shortcut to the closed testing procedure.

Theorem 5. *For every $V \subseteq M$, let*

$$\underline{\mathbf{a}}(V) = \sum_{i=1}^n \check{s}_{k_M}(\mathbf{C}_i),$$

where $\mathbf{C}_1, \dots, \mathbf{C}_n$ are disconnected clusters such that $\mathbf{C}_1 \cup \dots \cup \mathbf{C}_n = V \cap \mathbf{Z}$. Then, for all $P \in \Omega$,

$$P(\underline{\mathbf{a}}(V) \leq a_P(V) \text{ for all } V \subseteq M) \geq 1 - \alpha.$$

Computational complexity for $\underline{s}_k(V)$ is $O(|V|)$, and for $\check{s}(V)$ is $O(|V|^{1+1/d})$, so that is also the computational complexity of $\underline{\mathbf{a}}(V)$ if V is a supra-threshold cluster. For general V , complexity is the sum of the complexity of its comprising clusters, which is $O(|V|^{1+1/d})$ in the worst case that V is a supra-threshold cluster.

It is easy to verify that the shortcut of Theorem 5 also retains the property of Theorem 2 that it uniformly improves classic cluster inference. Still, it sacrifices some power, since the lower bound $\check{s}_k(V)$ may be (much) smaller than $s_k(V)$. The difference between $s_k(V)$ and $\check{s}(V)$ can be expected to be relatively large especially if $|V|/k$ is small and if V is irregularly shaped.

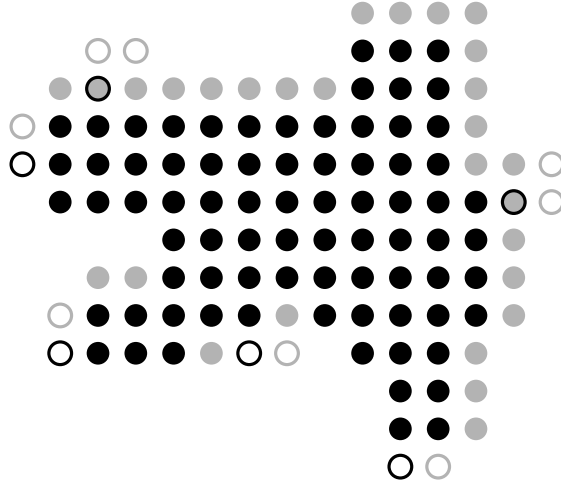


Figure 4: Illustration of the pruning V' of the voxel set V from Figure 2. The voxel set V consists of all black voxels (open and filled); the set V^+ additionally comprises of the gray voxels (open and filled). The pruned set $V' = (V^-)^+$ consists of the filled black voxels, and its cover $(V')^+$ of all filled grey voxels. We see that each voxel removed to obtain V' nets a reduction in size of 2 voxels for $(V')^+$, resulting in a net gain in $\underline{s}_k(V')$ relative to $\underline{s}_k(V)$, since $r_k \leq 1/2$.

5.7 Heuristic algorithms to minimize k -separators

The strength of the shortcut of the previous paragraph is its guaranteed TDP control, as expressed in Theorem 5. To obtain this control the shortcut sacrifices power in exchange for computational efficiency. In this section we present an alternative computational approach that aims to approximate $s_k(V)$ heuristically as closely as possible, instead of bounding it from below. The algorithm has two parts. First, a heuristic algorithm finds a good separator. Next, an attempt is made to find a local improvement of the solution using simulated annealing. The second phase of the algorithm uses Theorem 3.

The first heuristic algorithm finds clusterings with acceptable sizes of separator sets. The algorithm consists of two phases: inferring an initial clustering, and improving regions consisting of a small number of neighbouring clusters. In the first phase, the algorithm starts from an empty clustering. It generates a small number of candidate clusters, where the number is a small integer, usually between 1 and 10. Each candidate cluster is created starting from a randomly chosen available voxel by a sequence of insertions of adjacent voxels such that the induced size of its separator is kept small. Then, the best candidate cluster, i.e., the cluster with the separator's minimal size, is inserted into the current clustering. The procedure is repeated until there is no space to insert a new cluster. The second phase consists of repetitions of local improvements. The algorithm randomly takes a small number of neighbouring clusters, removes them from the current clustering, and applies a procedure similar to the first phase to find a better setting of clusters.

We follow up on the optimal heuristic separator using a simulated annealing algorithm, as follows. The separator of V is translated to a tiling of V^+ according to Lemma 4. In each step, the algorithm chooses a random voxel $v \in V^+$ and a random neighbor $w \in V^+$ of v . If v and w are part of the same tile T with interior size $|T^- \cap V| > k$, the algorithm proposes to start a new tile $\{v\}$; otherwise it proposes to reassign v from its old tile to the tile of w . If the target function t' of the proposed tiling is lower than or equal to the target function t of the previous step, the proposal is always accepted. Otherwise, the proposal is accepted with a probability that is a decreasing function of $t' - t$ and of the current iteration number. After a maximum number of iterations is reached, the algorithm returns the best solution it found during its travels through the search space.

The first algorithm was implemented in C and the simulated annealing in Python. The algorithms are usually

invoked with a time limit setting. Pseudo-code for both heuristic algorithms are given in the Supplemental Information, Section B.

The heuristic algorithms are not guaranteed to find the global minimum with a finite running time. If the algorithm did not find the correct solution, the value found is larger than the actual minimum $s_k(V)$, so there is no formal guarantee of TDP control comparable to Theorem 5. Still, the overstatement of $s_k(V)$ may often be less than the understatement of $s_k(V)$ due to the lower bound (4). The heuristic approach may therefore be the preferred solution in practice if computation time is not an issue and a small overstatement of TDP is acceptable.

5.8 Heuristic algorithm performance

A heuristic algorithm for a computationally hard problem cannot guarantee to find the optimal solution. Also estimating the error of such approaches is usually a difficult task. One way to proceed is to use exact solution approaches such as exhaustive enumeration, dynamic programming, or integer linear programming formulations. However, in the case of intractable problems, they can only be applied to small instances. Here, we propose a different approach. First, we show that some instances of the k -separator problem are tractable by showing their exact solution. Next, to estimate an error of the heuristic algorithm given the input consisting of multiple datasets, we generate a number of tractable instances matching properties of the input and jointly apply the heuristic algorithm under the same parameter setting. Finally, knowing the exact solution of tractable instances, we can estimate the solution error of the input datasets. The main result is formulated below in Lemma 7

Lemma 7. *Let $k = n^d$ and c be a vector of d positive integers. If the dimensions of a hyperrectangle R are $(n + 1)c_i - 1$ for $i = 1, \dots, d$, then the bound of Theorem 4 is exact, so that the optimal k -separator of R has $|R| - n^d \prod c_i$ voxels.*

Since our algorithm is not utilizing the information on the shape of the input voxel sets, nor the clusters are formed as cubes in the sampling, we believe that the benchmark of correctness based on hyperrectangles is a good indicator of how scores from the heuristic differ from the optimal ones.

To estimate the error of the heuristic algorithm, we inferred a collection of hyperrectangle tests based on the three-dimensional datasets from the Neurovault repository (see Section 10). Our goal was to cover the whole range of k values and datasets sizes from the input repository. Therefore, we set k bounded above 1000, and the hyperrectangle, i.e., cuboid, sizes to maximum 18000 voxels. Being consistent with the notation from Lemma 7, each test is uniquely determined by four integer parameters $n, c_1, c_2, c_3 \leq 10$, where k is n^3 , and the corresponding cuboid has dimensions $(n + 1)c_i - 1$, for each i . After rejecting too large cuboids, we obtained 1064 tests, which enlarged the input repository by nearly 9%.

The experiment indicated that nearly 50% of tests were completed with no error, and the worst errors of 5 – 6% has only $\sim 5\%$ of tests. A more detailed summary is depicted in Figure 5 with boxplots of errors for each value of k , where the 0% represents no error. The results obtained on cuboid tests indicate that the sizes of separators inferred by our heuristic algorithm are optimal in nearly half of the cases. For the rest of the cases, the error is usually below 4% with high confidence and the median error is below 2%.

6 Choosing thresholds

6.1 Voxel-wise inference

An alternative to cluster extent inference is classic voxel-wise inference. In voxel-wise inference, FWER is controlled over all voxel-wise null hypotheses. This is achieved by finding the $(1 - \alpha)$ -quantile of the distribution of the maximal z -score under the global null hypothesis H_M , and rejecting the null hypothesis whenever a voxel’s

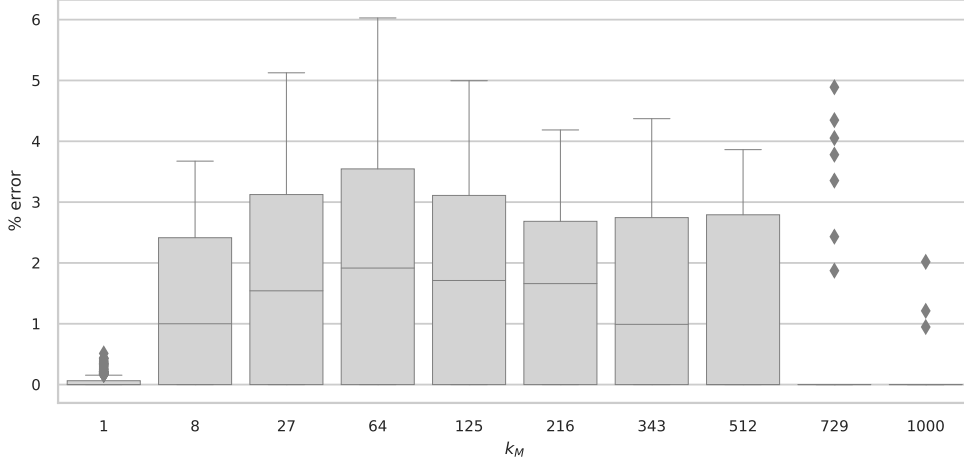


Figure 5: Upper bound heuristic performance: a boxplots of errors as a percentage of the true k -separator. Note that all errors are overestimates by construction.

z -score exceeds this threshold. Though cluster extent inference is often contrasted sharply with voxelwise inference, suggesting that these are two very different modes of operation. It was noted by Poline et al. (1997) and Friston et al. (1994) that classic voxelwise inference is simply a special case of cluster extent inference, obtained by choosing $k_M = 0$. It follows that we can get a TDP per cluster from voxelwise inference.

In classic voxelwise inference, we reject H_v for all voxels $v \in \mathbf{Z} = \{v \in M : \mathbf{z}_v \geq z\}$, where z is chosen as the smallest value such that

$$P(|M \cap \mathbf{Z}| > 0) \leq \alpha \quad (12)$$

holds for all $P \in H_M$. It has been shown (Worsley et al., 1992; Friston et al., 1991) that voxelwise inference controls voxelwise FWER, i.e., for all $P \in \Omega$,

$$P(\mathbf{Z} \not\subseteq A_P) \leq \alpha.$$

We can embed voxelwise inference into the closed testing procedure we have constructed by remarking that $|M \cap \mathbf{Z}| > 0$ if and only if $\chi_{M \cap \mathbf{Z}} > 0$. Therefore (12) is equivalent to

$$P(\chi_{M \cap \mathbf{Z}} > 0) \leq \alpha,$$

which is simply (2) with $k_M = 0$, and the latter is a valid choice for k_M . The closed testing procedure resulting from this choice is a relatively simple one, as the following theorem states.

Theorem 6. *If $k_M = 0$, then for all $V \subseteq M$ we have*

$$\underline{\mathbf{a}}(V) = \check{\mathbf{a}}(V) = \mathbf{a}(V) = |V \cap \mathbf{Z}|.$$

The theorem says how to calculate TDP for clusters when doing voxelwise inference: the TDP lower bound for a set V is simply the fraction of voxelwise significant voxels among the voxels in V . Supra-threshold clusters obtained with $k_M = 0$ always have a TDP of 100%.

6.2 Choosing k_M

Cluster extent inference assumes that z and k_M are chosen in such a way that (2) holds. It is common in cluster extent inference to fix the z -score threshold z , and to calculate k_M as the smallest value such that (2) is satisfied (Friston et al., 1994). However we saw in the previous section that the order is reversed in voxelwise inference: there $k_M = 0$ is fixed, and z is chosen as the smallest value of z satisfying (2). In this section, we argue that the order of fixing k_M calculating z should be generally preferred, both from the perspective of power and obtaining a good TDP bound.

It is perfectly valid to choose k_M first, and to find a value of z that corresponds to this k_M , as previously proposed by Bullmore et al. (1999). The relationship between z and k_M depends only on the null model H_M , and not on the observed z -scores. For cluster inference based on random field theory, the relationship between z and k_M depends on the smoothness of the field, which is estimated from the independent residuals. For cluster inference based on permutations, k_M is calculated from the matrix of all permutation z -scores, and can be calculated without knowing which permutation corresponds to the real data. We present a fast algorithm for finding z based on k_M using permutations in the Supplemental Information, Section E.

It is generally (slightly) more powerful to choose k_M rather than z . The reason for this is that k_M is discrete, while z is continuous. When fixing z and calculating k_M there is almost always a smaller value of z that would result in the same value of k_M . Using this value instead of the previously chosen z would result in a uniformly more powerful method but still controls TDP, since (2) still holds. We may therefore, after choosing z and finding k_M , always re-calibrate our z .

Alternatively, we may simply choose k_M and find z as the smallest value such that (2) holds, as is done in voxelwise inference. This has the important advantage that the achievable TDP can be better controlled.

7 Upper bounds

In this section we present two upper bound results that impose hard limits on the TDP that can be achieved with closed testing based on cluster extent inference. The first bound, in Section 6.2, limits what can be achieved using the lower bound; this result helps to choose the settings of that method. The second bound, in Section 7.1, limits what can be achieved in terms of TDP by the full closed procedure (6). Since closed testing procedures can only be uniformly improved by improving their local tests (Goeman et al., 2021), and that the room for such improvements is limited if (2) is tight, this sets a limit on the potential of any method that is consistent with classic cluster extent inference.

The maximal achievable TDP from the shortcut can be calculated as a function of k_M and cluster size $|\mathbf{C}|$ by the following theorem.

Theorem 7. *For every cluster $\mathbf{C} \subseteq \mathbf{Z}$, we have*

$$\underline{\mathbf{a}}(\mathbf{C}) \leq \left\lceil \frac{r_{k_M} - r_{|\mathbf{C}|}}{1 - r_{|\mathbf{C}|}} \cdot |\mathbf{C}| \right\rceil \vee \mathbf{1}\{|\mathbf{C}| > k_M\}.$$

By Theorem 7, to achieve a TDP of γ , for some $\gamma > 1/k_M$, we need a cluster \mathbf{C} with

$$r_{|\mathbf{C}|} \leq \frac{r_{k_M} - \gamma}{1 - \gamma}.$$

The maximal TDP according to $\underline{\mathbf{a}}$ for different values of k_M and different cluster size $|\mathbf{C}|$ is given in Figure 6. Since $r_{|\mathbf{C}|} \rightarrow 0$ as $|\mathbf{C}| \rightarrow \infty$, the TDP lower bound $\underline{\mathbf{a}}(\mathbf{C})/|\mathbf{C}|$ achieved by the shortcut of Theorem 5 is at most r_{k_M} for very large clusters, and much smaller than that for small and irregular clusters. The maximal TDP values converge to r_k as the cluster size increases. Clusters may achieve the maximal TDP if they are highly compact. Irregular clusters tend to have (much) smaller TDP.

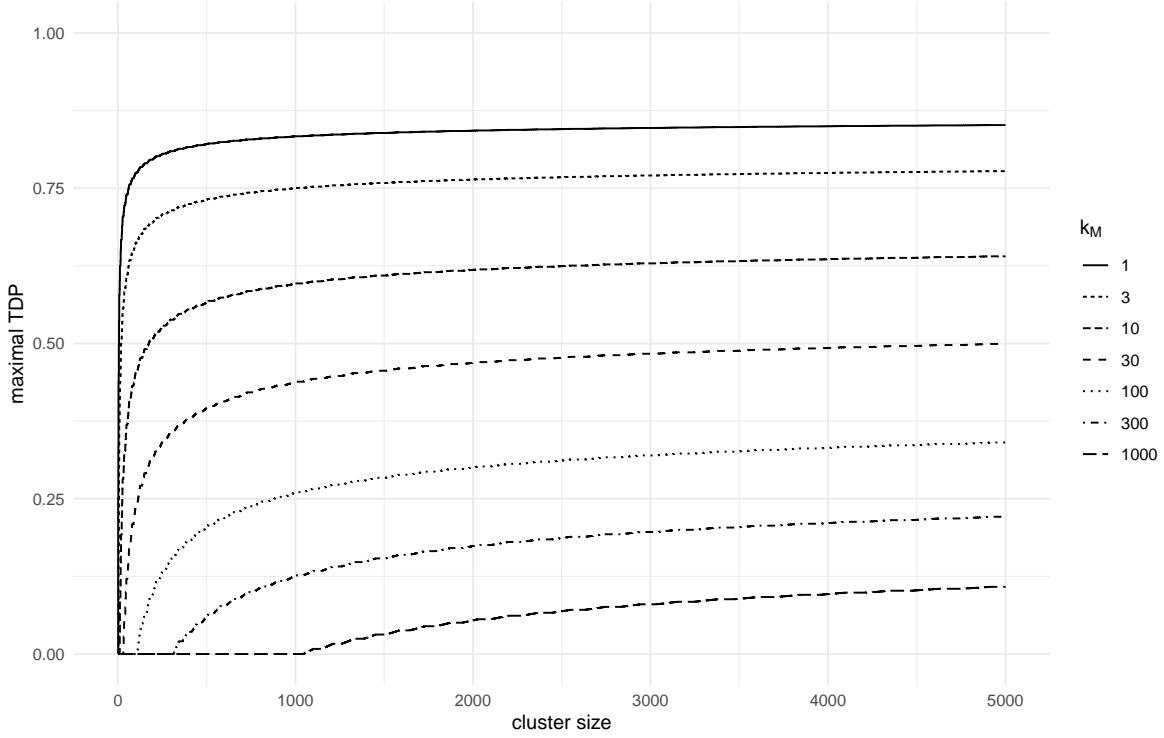


Figure 6: The maximal TDP according to the shortcut $\underline{a}(V)$, defined in Theorem 5, as a function of the extent threshold k_M and cluster size, for dimensions $d = 3$.

We see from Figure 6 that, with large values of k_M , it is difficult or even impossible to achieve good TDP even for large clusters, so a small value of k_M is recommended if large TDP is desired. Assuming that we are interested in finding clusters with $\text{TDP} \geq 1/2$, a sweet spot with $d = 3$ seems to be $k_M = 14$, for which $r_{k_M} = 2/3$. To achieve $\text{TDP} \geq 1/2$, clusters need to have $r_{|V|} \leq 1/3$, which implies $|V| \geq 339$.

For $\check{\mathbf{a}}(V)$ we have a weaker bound $\check{\mathbf{a}}(V) \leq \tilde{r}_{k_M} \cdot |V|$, from Lemma 8, below, that bounds TDP by $\tilde{r}_k \approx r_k$. The value of \tilde{r}_k is illustrated in Figure 3 in Section 5.5. This bound suggests that also when using the heuristic approximation to the k -separator problem, a researcher would want to use a value of k_M that yields \tilde{r}_{k_M} substantially above the target TDP. E.g., getting a TDP over 0.5 is impossible if $k_M > 64$, and remains unlikely unless k_M is substantially smaller than 64, since the bound of Lemma 8 is not very tight.

Lemma 8. *We have $s_k(V) \leq \tilde{r}_k \cdot |V|$, where $\tilde{r}_k = (b_{d,k}^+ - b_{d,k})/b_{d,k}^+$.*

Note that $b_{d,k}$ and $b_{d,k}^+$ are defined in Lemma 5.

7.1 The limits of cluster extent thresholding

In the previous section we considered upper bounds for the shortcuts to the closed testing procedure. Such bounds are useful for researchers intending to use these shortcuts. In this section we consider an upper bound to the full closed testing procedure (7), given below in Theorem 8. This bound is of fundamental and practical interest, as we will explain.

Theorem 8. *Let $\bar{\mathbf{a}}(V) = s_{k_M \setminus \mathbf{Z}}(V \cap \mathbf{Z})$, then, for every $V \subseteq M$,*

$$\mathbf{a}(V) \leq \bar{\mathbf{a}}(V).$$

In the proof of this theorem in the Supplemental information (Section A) we will prove a slightly tighter bound. Note the similarity of $\bar{\mathbf{a}}(V)$ with $\check{\mathbf{a}}(V)$, the only difference being that k_M is replaced by $k_{M \setminus \mathbf{Z}}$. This difference will be small unless $|\mathbf{Z}|$ is large relative to $|M|$.

Practically, Theorem 8 can be used to bound the loss $\mathbf{a}(V) - \underline{\mathbf{a}}(V)$ of the shortcut $\underline{\mathbf{a}}(V)$ relative to the full closed testing procedure $\mathbf{a}(V)$. It limits the potential for further computational improvements. In practice, unless $|\mathbf{Z}|$ is large relative to $|M|$ we will have $k_M \approx k_{M \setminus \mathbf{Z}}$, so that $\check{\mathbf{a}}(V) \approx \bar{\mathbf{a}}(V)$, and $\check{\mathbf{a}}(V) \approx \mathbf{a}(V)$.

More fundamentally, we can combine Theorem 8 with the insights from Goeman et al. (2021). We have constructed $\mathbf{a}(V)$ as the unique closed testing procedure induced by cluster extent inference. By Goeman et al. (2021) closed testing procedures are optimal, so there is no room for improvement of the method outside the closed testing framework. Moreover, improvement within the closed testing framework is limited to improvement of the local test, and there is hardly room for that if z and k_M are optimized for (2). It follows that Theorem 8 gives a clear upper bound to the TDP arising from any method that is based on cluster extent thresholding. Any method that achieves the result of Theorem 2 would also be constrained by the result of Theorem 8.

8 Simulation

In this section, Monte Carlo simulation is conducted to demonstrate the validity of our proposed methods, to investigate the tightness the TDP, and to see the gap between the upper and lower TDP bounds.

8.1 Set-up

2D images, each with 128×128 pixels, were simulated. Two spatial signal configurations were considered, shown in Figure 7: (1) a focal configuration with a single large circle of signal in the middle and (2) a distributed configuration with 9 small circular regions of signal spread out. The number of pixels with signal was 716 for both configurations. The simulated images were created by filling each pixel with spatially correlated noise, starting from i.i.d. standard Gaussian noise and smoothing with a spatial Gaussian smoothing kernel with full width at half maximum (FWHM) of 4 pixels, i.e., with $\sigma = 1.7$ pixels. Signal was added according to the chosen configuration at a fixed signal amplitude of $d = 0.1$ and $d = 0.05$, respectively. We considered 20 sample sizes n between 10 and 200 with an increment of 10, and a total of 1000 images were generated for each simulation setting. We calculated z -scores for each voxel using a one-sample t -test. Clusters of interest were defined as all connected components of \mathbf{Z} as defined in Section 3, using z -score thresholds $z = 0.348 \times \sqrt{n}$ for each sample size n .

To calculate the k_M threshold at $\alpha = 0.05$ fulfilling (2) we simulated a second independent null field without signal for each combination of each sample size and threshold, smoothed in the same way. We calculated k_M as the 95% quantile of the empirical distribution of the maximum cluster size in this null field. Clusters of size k_M or smaller were discarded in accordance with standard practice. Subsequently, the TDP bound was calculated using both the heuristic algorithm of Section 5.7 and the lower bound of Theorem 5.

8.2 Results

Figure 8 shows the average size of the clusters found, illustrating the qualitative difference between the two signal amplitudes. Here, the cluster size is standardized to a percentage based on the true signal size. At the high amplitude ($d = 0.1$) the clusters are consistent for the signal, with clusters converging to the true signal as the sample size increases. In contrast, at the low amplitude the clusters capture a vanishing fraction of the true signal.

Figure 9 shows the error rate of the method, which is well controlled at $\alpha = 0.05$ for all settings. The lower bound is conservative for large and for small sample sizes, while the heuristic algorithm is only conservative

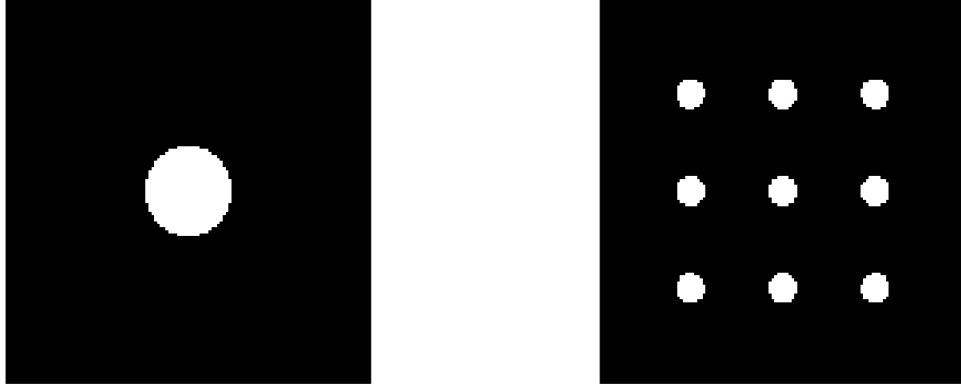


Figure 7: 2D simulated signal illustration. Focal signal (left) with one large circle in the middle; distributed signal (right) with nine identical circular regions.

for large sample size. We explain this for small sample size by the compactness of the chosen signal regions, for which the lower bound method tends to underestimate TDP. For large sample size, conservativeness is due to discreteness of k_M , so that the α -level in (2) is not exhausted. The heuristic algorithm also controls its error rate quite well in this simulation, despite the lack of a theoretical guarantee.

Figure 10 shows the TDP bounds found by the method. Displayed is the average value of the TDP over all significant clusters, i.e. over all clusters with $\text{TDP} > 0$. Note that the number of such clusters is much smaller for the low signal amplitude setting than for the high amplitude setting, and much larger for the distributed configuration of signal than for the focal one. We see that in all settings the TDP of significant clusters goes to 1 as sample size increases. This is because the value of k_M decreases with the sample size, eventually reaching $k_M = 0$. The difference in TDP between the lower bound and the heuristic algorithm is appreciable but not overly large, almost never exceeding 10%.

9 Application: Human Connectome Project n -back task revisited

We illustrate the use of the new method using a more extensive analysis of the data set introduced in Section 2.

A z -score threshold z and cluster extent threshold k_M can be defined in any way that satisfies (2); that is, fixing one threshold, the smallest value of the other still satisfying (2) can be calculated. We present the permutation-based thresholds in this Section, using the fast algorithm for finding z as a function of k_M using permutations given in the Supplemental Information, Section E. For comparison, the analysis with thresholds based on random field theory is given in the Supplemental Information, Section F.

We present two alternative permutation-based analyses. First, we fixed $z = 3.1$, which corresponds to $k_M = 72$ in this data (Table 2). Next, we fixed $k_M = 14$ and calculated the corresponding z -threshold $z = 3.7$ (Table 3). Non-significant supra-threshold clusters were not displayed. The TDP bounds for relevant overlapping anatomical regions are also displayed.

TDP was calculated both using heuristic algorithms and using the lower bound of Theorem 5. Our heuristic algorithms were run for several hours on a cluster to produce these results, and we believe that these results are sufficiently close to the true minimum. Shorter running times of 20–60 seconds would give TDP results up to only 5% higher than the reported values. Comparing the heuristic results and the lower bound, the lower bound was closest to the heuristic solution for large clusters and small k_M , as expected from the theory.

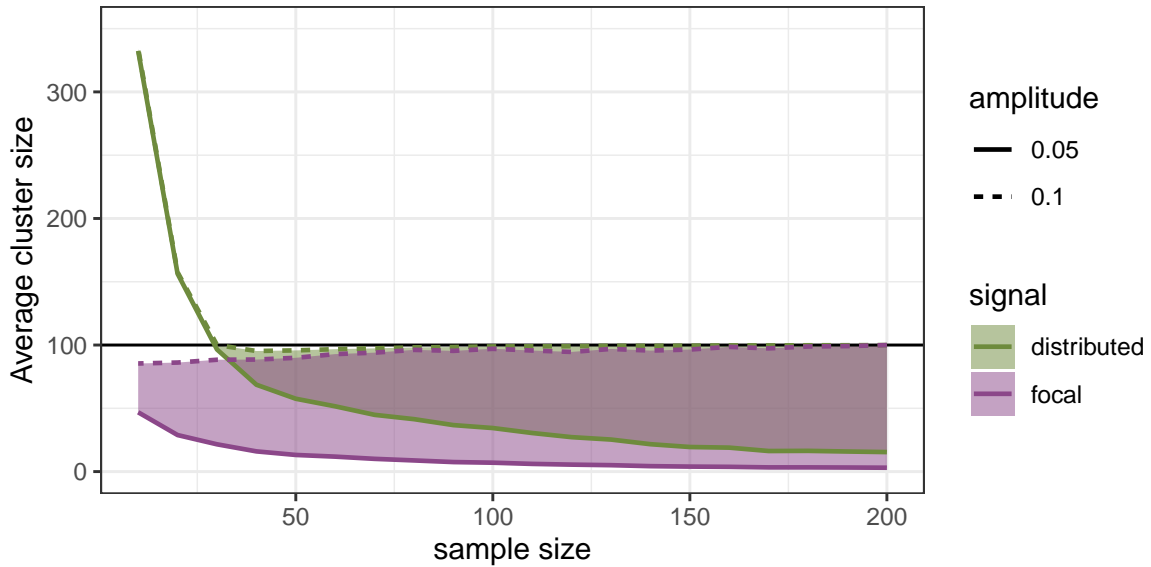


Figure 8: Average cluster sizes (standardized and expressed in percent) for focal (purple) and distributed (green) signals with the amplitudes of $d = 0.1$ (dashed line) and $d = 0.05$ (solid line).

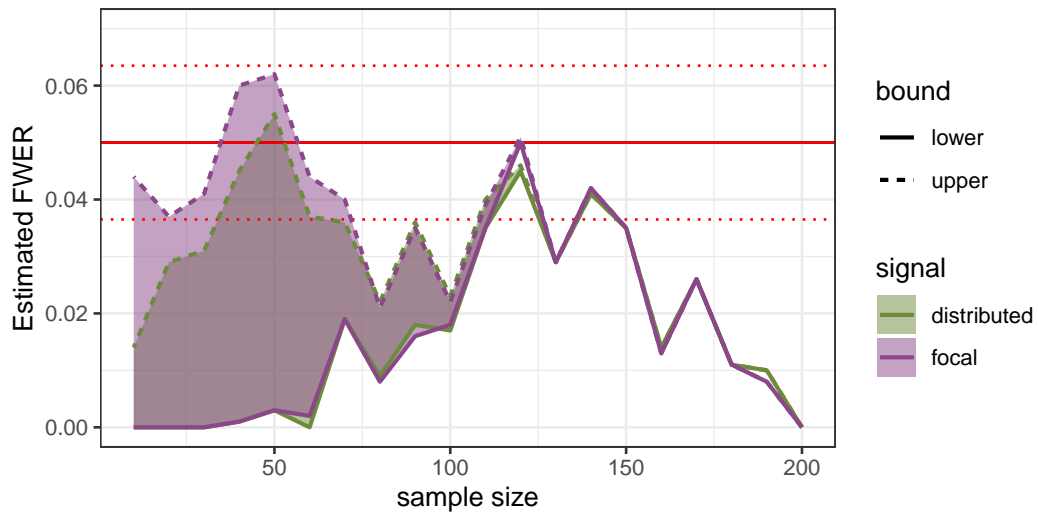
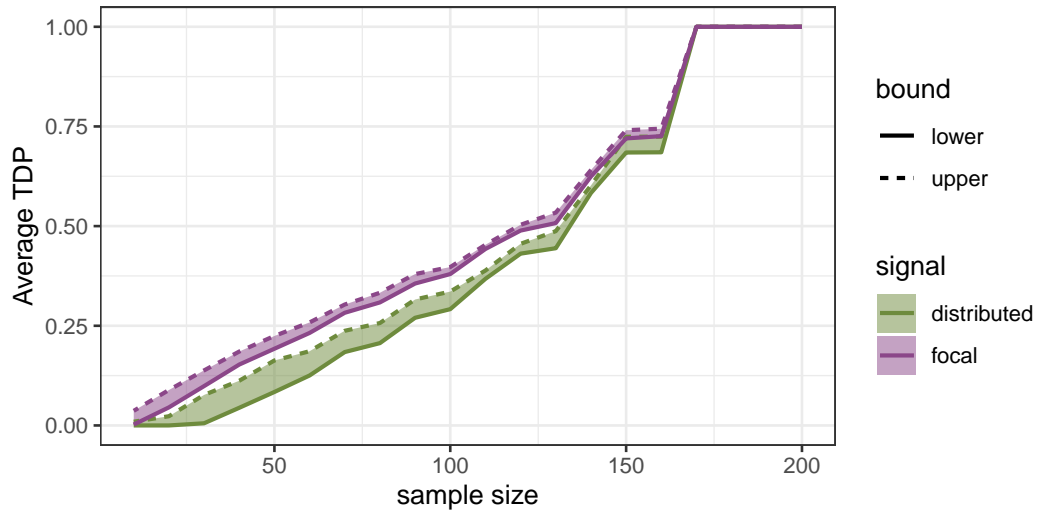
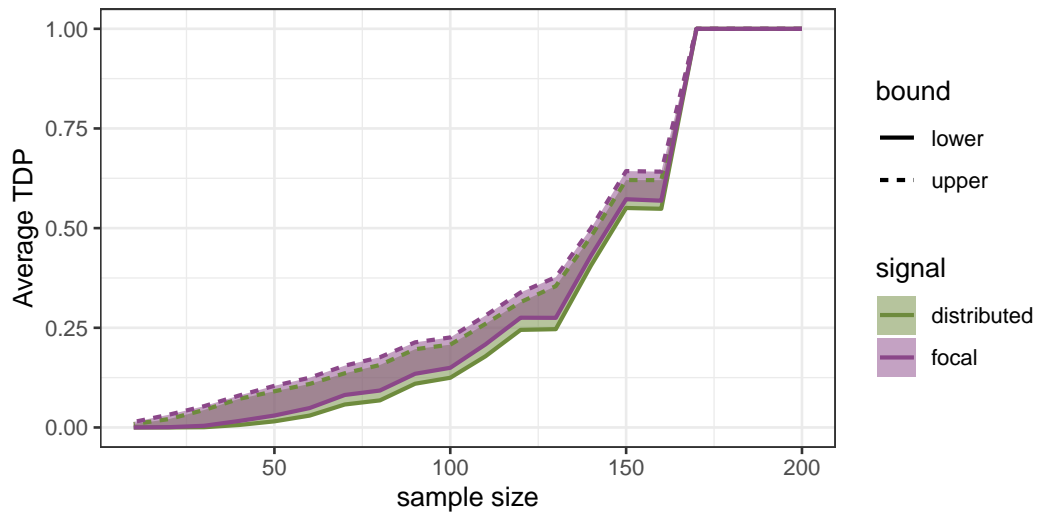


Figure 9: Estimated family-wise error rates (FWER) for focal (purple) and distributed (green) signals with the amplitudes of $d = 0.1$. The red dotted horizontal lines represent the binomial confidence intervals for the FWER at $\alpha = 0.05$ (solid horizontal line). Shown are the results for lower-bound (solid line) and upper-bound (dashed line) based on the heuristic algorithm. The results for $d = 0.05$ (not shown) are almost identical, since the same realization of the noise field was used for both simulations.



(a) high signal amplitude of $d = 0.1$.



(b) low signal amplitude of $d = 0.05$.

Figure 10: Average TDP bounds for all significant clusters for focal (purple) and distributed (green) signals with the amplitudes of $d = 0.1$ and $d = 0.05$. Shown are the results for lower-bound (solid line) and upper-bound (dashed line) based on the heuristic algorithm.

Comparing the $z = 3.1$ and $k_M = 14$ settings, the results clearly show a trade-off between detection and TDP. The lower cluster extent threshold k_M , that corresponds to a higher z -threshold, returns smaller clusters with larger TDP, while the high k_M results in larger clusters with smaller TDP. For anatomical regions it is not a priori clear whether larger TDP would be found with high or low values of k_M . In this data set, increased TDP bounds were perceived when k_M was small, i.e. when the z -threshold was large. Corresponding anatomical regions of the clusters were identified using the Harvard-Oxford cortical structural atlas and MNI structural atlas as available in FSL (Jenkinson et al., 2012).

Table 2: Results for supra-threshold clusters, defined by the cluster-forming z -threshold of $Z > 3.1$ and the resulting minimal cluster extent threshold $k_M = 72$ based on permutation. The results from the heuristic algorithms are indicated by TDP, the lower bound of Theorem 5 by LB.

Cluster				Anatomical region					Location							
ID	size	TDP	LB	Region	size	overlap	TDP	LB	x	y	z	Z_{\max}				
1	8870	0.368	0.265	MFG	18250	4049	0.082	0.061	44	72	60	8.87				
				FP	33571	2021	0.020	0.013								
				IC	6591	564	0.025	0.016								
2	8526	0.402	0.307	sLOC	27121	5142	0.069	0.049	19	42	61	9.51				
				AG	13689	4260	0.117	0.089								
				pSMG	14829	3804	0.097	0.074								
				Precuneous	18119	2491	0.051	0.037								
3	7956	0.332	0.201	Cerebellum	39724	6551	0.057	0.037	63	33	20	9.20				
4	6652	0.372	0.265	MFG	18250	4035	0.083	0.061	31	67	64	9.73				
				FP	33571	2587	0.026	0.018								
				IC	6591	589	0.026	0.017								
5	350	0.191	0.037	pMTG	11420	310	0.006	0.001	15	46	28	5.18				
				tMTG	9735	271	0.005	0.000								
6	100	0.140	0.010	Cerebellum	39724	100	0.000	0.000	49	35	10	6.56				
				Total	32454	0.367	0.257	MFG					18250	8084	0.165	0.122
				Cerebellum	39724	6651	0.058	0.037								
				sLOC	27121	5142	0.069	0.049								
				FP	33571	4608	0.046	0.031								
				AG	13689	4260	0.117	0.089								
				pSMG	14829	3804	0.097	0.074								
				Precuneous	18119	2491	0.051	0.037								
				IC	6591	1153	0.051	0.033								
				pMTG	11420	310	0.006	0.001								
tMTG	9735	271	0.005	0.000												

10 Application: Neurovault

Next, we applied the new algorithm to a selection of 818 datasets from the Neurovault database (neurovault.org; Gorgolewski et al. (2015)). The Neurovault database consists of unthresholded maps from neuroimaging studies. We selected 818 representative functional MRI datasets containing group-level statistics maps. For the calculation of clusters we used two settings: a standard z -threshold of $z = 3.1$, and a k -threshold of $k_M = 14$.

Table 3: Results for supra-threshold clusters, defined by cluster extent threshold $k_M = 14$ and the resulting cluster-forming z -threshold of $Z > 3.7$, based on permutation. The results from the heuristic algorithms are indicated by TDP, the lower bound of Theorem 5 by LB.

Cluster				Anatomical region					Location			
ID	size	TDP	LB	Region	size	overlap	TDP	LB	x	y	z	Z_{\max}
1	7231	0.606	0.532	sLOC	27121	4293	0.091	0.078	19	42	61	9.51
				Precuneous	18119	2123	0.067	0.058				
2	6899	0.577	0.487	MFG	18250	3224	0.102	0.087	44	72	60	8.87
				SFG	18946	2880	0.085	0.073				
				PCG	9245	1558	0.096	0.084				
				IC	6591	494	0.040	0.034				
3	5345	0.546	0.438	Cerebellum	39724	4840	0.067	0.054	63	33	20	9.20
4	5143	0.575	0.487	MFG	18250	3285	0.104	0.089	31	67	64	9.73
				FP	33571	1893	0.031	0.026				
				SFG	18946	1745	0.052	0.043				
5	202	0.391	0.158	OP	15486	156	0.004	0.001	39	22	36	5.72
				ICC	7134	110	0.006	0.003				
6	128	0.375	0.148	pMTG	11420	128	0.004	0.002	15	46	28	5.18
7	66	0.379	0.182	Cerebellum	39724	66	0.001	0.000	49	35	10	6.56
8	61	0.361	0.115	FP	33571	61	0.001	0.000	31	86	29	5.77
9	56	0.321	0.143	FP	33571	56	0.001	0.000	57	88	29	5.16
10	39	0.308	0.103	OP	15486	39	0.001	0.000	51	15	42	5.35
11	22	0.182	0.045	Thalamus	4602	17	0.000	0.000	43	53	43	4.55
12	21	0.095	0.048	Cerebellum	39724	21	0.000	0.000	42	36	10	4.85
Total	25213	0.573	0.482	MFG	18250	6509	0.206	0.176				
				Cerebellum	39724	4927	0.068	0.054				
				SFG	18946	4625	0.137	0.116				
				sLOC	27121	4293	0.091	0.078				
				Precuneous	18119	2123	0.067	0.058				
				FP	33571	2010	0.032	0.026				
				PCG	9245	1558	0.096	0.084				
				IC	6591	494	0.040	0.034				
				OP	15486	195	0.004	0.001				
				pMTG	11420	128	0.004	0.002				
				ICC	7134	110	0.006	0.003				
				Thalamus	4602	17	0.000	0.000				

The corresponding k_M - and z -thresholds, respectively, were estimated using Gaussian Random Field Theory (Forman et al., 1995). As residual data were unavailable, we estimated smoothness of the random field on the z -statistics image. The $z = 3.1$ setting produced values of k_M ranging from 71 to 507 (1st and 9th decile). Details of the selected images and estimation procedures can be found in the Supplemental Information, Section D.

For each dataset we estimated the TDP of each supra-threshold cluster obtained using $z = 3.1$ and $k_M = 14$. We then calculated for each TDP value how many supra-threshold voxels with at least that TDP were significant

on average across all datasets. This allows us to visualize the relationship between the size of the clusters detected and the TDP of those clusters for different methods. We plot the theoretical lower-bound of both methods (according to Theorem 5), and the solution as estimated using the heuristic methods. For reference we also calculated the number of voxels above the Gaussian random field voxelwise threshold (equivalent to a $k_M = 0$ setting).

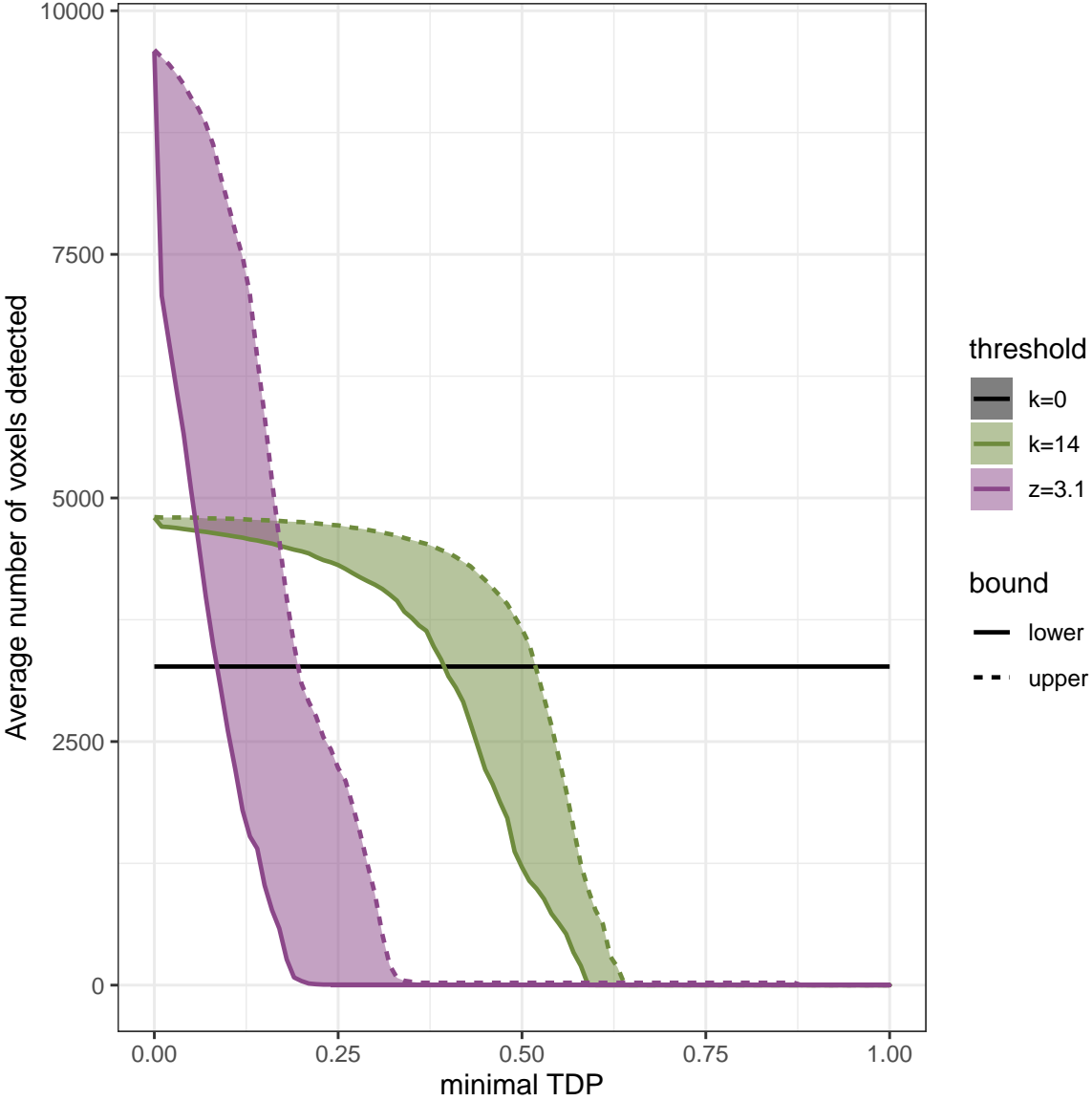


Figure 11: Relation between TDP (x -axis) and the average number of voxels detected for three thresholds: $z = 3.1$ (purple), $k_M = 14$ (green), and $k_M = 0$ (black). The results for lower-bound (solid line) and upper-bound (dashed line) are shown based on the heuristic algorithm.

Figure 11 shows the results of the analysis across all datasets. As can be seen the $z = 3.1$ setting (purple) leads to larger cluster sizes but with low TDP's. For $k_M = 14$ (green), the size of the clusters with low TDP's is smaller, but there are more clusters with a more reasonable (albeit still relatively small) TDP. Both methods

detect larger regions than voxelwise inference ($k_M = 0$, black line) at low TDP thresholds, but smaller regions at high TDP. The figure shows a clear trade-off between detection and TDP: at low k_M settings, small regions are detected with large TDP; with high k_M , larger regions are detected, but TDP is (much) lower.

We note that the estimation of the smoothness using the z -statistics rather than the residuals tends to overestimate the smoothness if there is much signal. As a result, it is likely that we have overestimated values of k_M when $z = 3.1$ and overestimated z when $k_M = 14$. The TDP results in Figure 11 are therefore likely an underestimate of what would be found if the full datasets would have been available.

11 Discussion

We have presented a uniform improvement of classic cluster inference that allows much more meaningful and informative inference to be obtained from that method. In the first place, the new method allows inference on anatomical regions of interest and data-driven supra-threshold clusters within the same analysis. Moreover, regions of interest do not have to be specified before seeing the data. Secondly, rather than (only) a p -value, the new method provides a true discovery proportion (TDP) for every brain region. Quantifying the spatial extent of activation within the brain region, the TDP is much more informative than the p -value, which only quantifies the evidence for the presence of any signal at all. TDP is also less prone to overinterpretation than the p -value. In the Neurovault analysis we have found many examples of brain regions with a seemingly impressive $p < 0.001$ that had unremarkable TDPs of 20% or less. We recommend that TDP is always reported with (or even instead of) the p -value in fMRI cluster inference.

Despite making these additional inferences, error control remains as strict as with classic cluster inference: with probability at least $1 - \alpha$ no regions get an estimated TDP that is larger than the true value. To guarantee this error control, the method does not require any additional model assumptions. It can assume either that the z -scores of inactive voxels follow a Gaussian random field or that they are invariant under permutations.

Inference on brain regions in terms of TDP can be said to solve the Spatial Specificity Paradox (Woo et al., 2014), but by doing so it makes the same paradox painfully visible. At the usual setting with a cluster-forming threshold of $z = 3.1$ most significant brain regions have a TDP less than 20–30%. Our analyses have made it clear that there is a trade-off involved in choosing the cluster-forming threshold. Low thresholds result in many large clusters but with low TDP; higher thresholds have less detection power but much higher TDP. In the extreme, voxel-wise inference was shown to be a special case of cluster extent inference that always returns a TDP of 100%. In order to obtain TDP substantially over a reasonably minimal threshold of 50%, we recommend cluster thresholding with $k_M = 14$ or less, resulting in much larger z -thresholds than usually recommended in the field (Eklund et al., 2016).

Computationally, the calculation of the TDP involves solving a k -separator problem. We presented two solutions to this problem: the lower bound retains the error control guarantee but is conservative; the heuristic solution is more accurate, but at the cost of losing error control if the method does not fully converge. Together, the two algorithms can be used to bracket the TDP lower confidence bound. We recommend the heuristic solution in practice provided enough computing power is available.

Inference for neuroimaging in terms of TDP rather than p -values has been proposed by several authors (Rosenblatt et al., 2018; Blanchard et al., 2020; Andreella et al., 2020; Vesely et al., 2021). None of the proposed methods is expected to outperform any of the others uniformly (Goeman et al., 2021). A systematic and careful inventory should be performed to find out when to prefer which TDP methods with which tuning parameters. This large project is beyond the scope of this paper. In such a comparison, the method proposed in this paper will serve as an important benchmark, representing classic cluster analysis, which it is designed to be consistent with.

Acknowledgements

Data were provided in part by the Human Connectome Project, WU-Minn Consortium (Principal Investigators: David Van Essen and Kamil Ugurbil; 1U54MH091657) funded by the 16 NIH Institutes and Centers that support the NIH Blueprint for Neuroscience Research; and by the McDonnell Center for Systems Neuroscience at Washington University. This research was supported by Nederlandse Organisatie voor Wetenschappelijk Onderzoek, Grant Number: 639.072.412.

A Proofs of Theorems and Lemmas

A.1 Proof of Lemma 1

Lemma 1. *For every $V \subseteq M$, we have $\underline{\psi}_V \leq \psi_V$.*

Proof.

$$\begin{aligned}
 \psi_V &= \min\{\phi_W : V \subseteq W \subseteq M\} \\
 &= \min\{\mathbb{1}\{\chi_{V \cap \mathbf{Z}} > k_V\} : V \subseteq W \subseteq M\} \\
 &\geq \mathbb{1}\{\min\{\chi_{V \cap \mathbf{Z}} : V \subseteq W \subseteq M\} > \max\{k_V : V \subseteq W \subseteq M\}\} \\
 &= \mathbb{1}\{\chi_{V \cap \mathbf{Z}} > k_M\} \\
 &= \underline{\psi}_V.
 \end{aligned}$$

□

A.2 Proof of Theorem 1

Theorem 1. *Let $\check{\mathbf{a}}(V) = s_{k_M}(V \cap \mathbf{Z})$, where $s_k(V) = \min\{|R| : \chi_{V \setminus R} \leq k\}$. Then, for all $P \in \Omega$,*

$$P(\check{\mathbf{a}}(V) \leq a_P(V) \text{ for all } V \subseteq M) \geq 1 - \alpha.$$

Proof. The minimum in (8) is achieved when $R \cap \mathbf{Z} = \emptyset$, so we can rewrite

$$\check{\mathbf{a}}(V) = \min\{|R| : R \subseteq V, \chi_{\mathbf{Z} \cap (V \setminus R)} \leq k_M\}.$$

Setting $W = V \setminus R$, we obtain

$$\begin{aligned}
 \check{\mathbf{a}}(V) &= \min\{|V \setminus W| : W \subseteq V, \chi_{\mathbf{Z} \cap W} \leq k_M\} \\
 &= \min\{|V \setminus W| : W \subseteq V, \underline{\psi}_W = 0\} \\
 &\leq \min\{|V \setminus W| : W \subseteq V, \psi_W = 0\} \\
 &= \mathbf{a}(V),
 \end{aligned}$$

where the inequality uses Lemma 1. The result now follows from (7). □

A.3 Proof of Theorem 2

Theorem 2. *If $\mathbf{C} \subseteq (\mathbf{Z} \cap M)$, with $|\mathbf{C}| > k_M$, is a cluster, then $\check{\mathbf{a}}(\mathbf{C}) > 0$.*

Proof. For $R = \emptyset$, we have

$$\chi_{(\mathbf{Z} \cap \mathbf{V}) \setminus R} = \chi_{\mathbf{Z} \cap \mathbf{V}} = \chi_{\mathbf{V}} = |\mathbf{V}| > k_M,$$

so the minimum in (8) is attained when $|R| > 0$. □

A.4 Proof of Lemma 2

We first state, perhaps superfluously, that smaller voxel sets contain smaller clusters.

Lemma 9. *If $V \subseteq W$, then $\chi_V \leq \chi_W$.*

Proof. Let $C \subseteq V$ be the largest cluster in V , then $C \subseteq V \subseteq W$ is a cluster in W . We have

$$\chi_V = |C| \leq \chi_W.$$

□

Lemma 2. *If $V = C_1 \cup \dots \cup C_n$, where C_1, \dots, C_n are disconnected clusters, then*

$$s_k(V) = \sum_{i=1}^n s_k(C_i).$$

Proof. Suppose R is an optimal k -separator of V , so that $\chi_{V \setminus R} \leq k$ and $s_k(V) = |R|$. For $i = 1, \dots, n$, define $R_i = R \cap C_i$. Since $C_i \setminus R_i \subseteq V \setminus R$, we have, by Lemma 9,

$$\chi_{V_i \setminus R_i} \leq \chi_{V \setminus R} \leq k,$$

so R_i separates C_i . Since R_1, \dots, R_n are disjoint, we have

$$s_k(V) = |R| = \sum_{i=1}^n |R_i| \geq \sum_{i=1}^n s_k(C_i).$$

Vice versa, suppose for $i = 1, \dots, n$ that R_i is an optimal k -separator of C_i , so that $\chi_{C_i \setminus R_i} \leq k$ and $s_k(C_i) = |R_i|$. Define $R = R_1 \cup \dots \cup R_n$. Let C be any cluster in $V \setminus R$. Since C_1, \dots, C_n are disconnected, we must have $C \subseteq C_i$ for some $1 \leq i \leq n$. We have

$$\chi_{V \setminus R} \leq \max_{1 \leq i \leq n} \chi_{C_i \setminus R_i} \leq k,$$

so R separates V . Since R_1, \dots, R_n are disjoint, we have

$$\sum_{i=1}^n s_k(C_i) = \sum_{i=1}^n |R_i| = |R| \geq s_k(V).$$

□

A.5 Proof of Lemma 3

We start with a lemma that is the reason the positive neighbors definition is so useful: two voxels are neighbors if and only if they have a positive neighbor in common.

Lemma 10. *Voxels $v, w \in \mathbb{Z}^d$ are neighbors if and only if $\{v\}^+ \cap \{w\}^+ \neq \emptyset$.*

Proof. Suppose v and w are neighbors. Consider $u = w + (v - w)_+$. Note that $x + (-x)_+ = x_+$. Then

$$u_i - v_i = (w_i - v_i) + (v_i - w_i)_+ = (w_i - v_i)_+ \in \{0, 1\},$$

so $u \in \{v\}^+$, and $u_i - w_i = (v_i - w_i)_+ \in \{0, 1\}$, so $u \in \{w\}^+$. Therefore $u \in \{v\}^+ \cap \{w\}^+ \neq \emptyset$.

Next, suppose that $u \in \{v\}^+ \cap \{w\}^+$. Then $u = v + e$ and $u = w + h$, with $e, h \in \{0, 1\}^d$. We have $v_i - w_i = h_i - e_i \in \{-1, 0, 1\}$, so v and w are neighbors. □

The next lemma translates the previous lemma to voxel sets: two voxel sets are disconnected if and only if their cover is disjoint.

Lemma 11. *Voxel sets $V, W \subseteq \mathbb{Z}^d$ are disconnected if and only if V^+ and W^+ are disjoint.*

Proof. Suppose V and W are not separated. Then there exist $v \in V$ and $w \in W$ that are neighbors. By Lemma 10 there exists $u \in \{v\}^+ \cap \{w\}^+$. By definition of V^+ and W^+ , we have $u \in V^+ \cap W^+$, so V^+ and W^+ are not disjoint.

Suppose V^+ and W^+ are not disjoint. Then $u \in V^+ \cap W^+$ exists. By definition of V^+ and W^+ there exist $v \in V$ and $w \in W$ such that $u \in \{v\}^+ \cap \{w\}^+$. By Lemma 10, v and w are neighbors, so V and W are not disconnected. \square

The cover and interior operations are not each other's inverse: the cover of the interior may be a smaller voxel set.

Lemma 12. $(V^-)^+ \subseteq V$.

Proof. Choose $v \in (V^-)^+$. By definition of the cover there must be a $w \in V^-$ such that $v \in \{w\}^+$. By definition of the interior, every positive neighbor of every $w \in V^-$ is in V . Therefore $v \in V$. \square

Now we come to proof of the lemma itself.

Lemma 3. *For every tiling T_1, \dots, T_n of V^+ there exists a k -separator R of V such that*

$$|R| = t_k(T_1, \dots, T_n).$$

Proof. For $i = 1, \dots, n$, let $R_i = T_i^0 \cap V$ and let R'_i be any subset of $T_i^- \cap V$ with $|R'_i| = (|T_i^- \cap V| - k)_+$. Then $R = R_1 \cup \dots \cup R_n \cup R'_1 \cup \dots \cup R'_n$ has $|R| = t_k(T_1, \dots, T_n)$.

We show that R is a k -separator of V . For $i = 1, \dots, n$, let $C_i = (T_i^- \cap V) \setminus R'_i$. Then $C_i \cap R = \emptyset$ and $V = R \cup C_1 \cup \dots \cup C_n$. Moreover, $|C_i| \leq k$ by definition of R'_i . Since $C_i \subseteq T_i^-$, we have $C_i^+ \subseteq T_i$ by Lemma 12. Therefore C_1^+, \dots, C_n^+ are disjoint. By Lemma 11, C_1, \dots, C_n are disconnected. It follows that

$$\chi_{V \setminus R} \leq \max_{1 \leq i \leq n} |C_i| \leq k,$$

so R is a k -separator of V . \square

A.6 Proof of Lemma 4

Lemma 4. *For every k -separator R of V there exists a tiling T_1, \dots, T_n of V^+ such that T_1, \dots, T_n are clusters, and*

$$|R| \geq t_k(T_1, \dots, T_n).$$

Proof. We write $V \setminus R = C_1 \cup \dots \cup C_n$ with C_1, \dots, C_n non-empty disconnected clusters. Since R is a k -separator of V , we have $|C_i| \leq k$ for $i = 1, \dots, n$. For $i = 1, \dots, n$ call $T_i = C_i^+ \subseteq V^+$. These are clusters since C_1, \dots, C_n are. Write

$$V^+ \setminus (T_1 \cup \dots \cup T_n) = T_{n+1} \cup \dots \cup T_{n+m},$$

with T_{n+1}, \dots, T_{n+m} disjoint clusters, so that $V^+ = T_1 \cup \dots \cup T_{n+m}$. Call $C_{n+1} = \dots = C_{n+m} = \emptyset$.

We will show that $t_k(T_1, \dots, T_{n+m}) \leq |R|$. Since $C_i \subset T_i$ for all $1 \leq i \leq n+m$, $v \in T_i^- \cap V \subseteq T_i$ cannot be in C_j for $j \neq i$, so $T_i^- \cap V \subseteq C_i \cup R$. Since C_i and R are disjoint, $(T_i^- \cap V) \setminus R = C_i$. Therefore,

$$|T_i^- \cap R| \geq |(T_i^- \cap V) \cap R| = |T_i^- \cap V| - |C_i| \geq (|T_i^- \cap V| - k)_+.$$

If $v \in C_i$, then $\{v\}^+ \subseteq C_i^+ = T_i$, so $v \notin T_i^0$. It follows that $T_i^0 \cap V = T_i^0 \cap R$ for $i = 1, \dots, n$. The same holds by definition for $i = n+1, \dots, n+m$. We have

$$\begin{aligned} |R| &= \sum_{i=1}^{n+m} |T_i^0 \cap R| + \sum_{i=1}^{n+m} |T_i^- \cap R| \\ &\geq \sum_{i=1}^{n+m} |T_i^0 \cap V| + \sum_{i=1}^{n+m} (|T_i^- \cap V| - k)_+ \\ &= t_k(T_1, \dots, T_{n+m}). \end{aligned}$$

□

A.7 Proof of Theorem 3

Theorem 3. *We have*

$$s_k(V) = \min\{t_k(T_1, \dots, T_n) : T_1, \dots, T_n \text{ is a tiling of } V^+\}.$$

The minimum is attained for a tiling for which T_1, \dots, T_n are all clusters.

Proof. Suppose R is a k -separator of V with $|R| = s_k(V)$. Then by Lemma 4 a tiling T_1, \dots, T_n exists such that $t_k(T_1, \dots, T_n) \leq |R| = s_k(V)$. It follows that

$$s_k(V) \geq \min\{t_k(T_1, \dots, T_n) : T_1, \dots, T_n \text{ is a tiling of } V^+\}.$$

Now suppose that T_1, \dots, T_n minimizes $t_k(T_1, \dots, T_n)$. By Lemma 3, a k -separator exists such that $|R| = t_k(T_1, \dots, T_n)$. It follows that

$$s_k(V) \leq \min\{t_k(T_1, \dots, T_n) : T_1, \dots, T_n \text{ is a tiling of } V^+\}.$$

Combining the two inequalities, the result follows. By Lemma 4 the optimal tiling can be taken as one that consists of clusters. □

A.8 Proof of Theorem 4

Though Theorem 3 allows tilings with a tile interior $> k$, we can always find an alternative solution that does not have such tiles.

Lemma 13. *Suppose T_1, \dots, T_n is a tiling of V^+ . Then there exists a tiling $T'_1, \dots, T'_{n'}$ with $t_k(T_1, \dots, T_n) = t_k(T'_1, \dots, T'_{n'})$ and $|T_i^-| \leq k$ for $i = 1, \dots, n'$.*

Proof. Choose any i such that $|T_i^-| > k$. We will construct T'_i and T'_{n+1} such that $T'_i \cup T'_{n+1} = T_i$, and $|(T'_i)^-| = |T_i^-| - 1$ and $(T'_{n+1})^- = 0$. Repeatedly applying this construction for all tiles with $|T_i^-| > k$ will give us the tiling with the desired property since the newly constructed tiling has the same value of t_k , but the interior of tile T_i is reduced in size by 1.

Choose any $v \in T_i^-$ that minimizes $\sum_{i=1}^d v_i$. Define $T'_i = T_i \setminus \{v\}$. Then all negative neighbors of v are not in $(T'_i)^-$, so

$$(T'_i)^- = T_i^- \setminus \{w \in T_i^+ : v \in \{w\}^+\}.$$

Let $w \in \mathbb{Z}^d$ such that $v \in \{w^+\}$. Then either $w = v$ or $v = w + e$ with $e \in \{0, 1\}^d$ and $\sum_{i=1}^d e_i \geq 1$. If $w \neq v$, then

$$\sum_{i=1}^d w_i = \sum_{i=1}^d v_i - \sum_{i=1}^d e_i \leq \sum_{i=1}^d v_i - 1,$$

so $w \notin T_i^-$ since v minimized $\sum_{i=1}^d v_i$ among $v \in T_i^-$. Therefore $\{w \in T_i^+ : v \in \{w\}^+\} = \{v\}$ and $(T_i^+)^- = T_i^- \setminus \{v\}$. So $|(T_i^+)^-| = |T_i^-| - 1$. Defining $T_{n+1}^+ = \{v\}$, we have $(T_{n+1}^+)^- = \emptyset$. This gives the required construction. \square

If the interior of the cover of a voxel set V is no larger than the original object, then the interior of all its tiles is in V .

Lemma 14. *If $(V^+)^- \subseteq V$, then for every $T \subseteq V^+$, we have $T^- \subseteq V$.*

Proof. Since $T \subseteq V^+$, we have $T^- \subseteq (V^+)^- \subseteq V$. \square

The next lemma is a special case of a property that holds in general for closed testing procedures (Goeman et al., 2021, Lemma 3). We prove it in context here.

Lemma 15. *If $V, W \subseteq \mathbb{Z}^d$ are disjoint, then $s_k(V \cup W) \leq s_k(V) + |W|$.*

Proof. Let R be a k -separator of V such that $|R| = s_k(V)$. Consider $R' = R \cup W$ and let C any cluster in $(V \cup W) \setminus R'$. Since $(V \cup W) \setminus R' = V \setminus R$, C is also a cluster in $V \setminus R$, so $|C| \leq k$, because R is a k -separator of V . Therefore, R' is a k -separator of $V \cup W$, and we have

$$s_k(V \cup W) \leq |R'| = |R| + |W| = s_k(V) + |W|.$$

\square

Theorem 4.

$$s_k(V) \geq r_k \cdot |V^+| - |V^+ \setminus V|,$$

where

$$r_k = \min\{|V^0|/|V| : \emptyset \neq V \subset \mathbb{Z}^d, |V^-| \leq k\}.$$

Proof. We first consider the special case that V fulfils $(V^+)^- \subseteq V$. In that case, let T_1, \dots, T_n be a tiling that minimizes $t_k(T_1, \dots, T_n)$. By Lemma 13, we can assume that $|T_i^- \cap V| \leq k$. By Lemma 14 we have $T_i^- \subseteq V$. Therefore $|T_i^-| \leq k$. We have

$$\begin{aligned} s_k(V) &= \sum_{i=1}^n |T_i^0 \cap V| + \sum_{i=1}^n (|T_i^- \cap V| - k)_+ \\ &= \sum_{i=1}^n |T_i^0 \cap V| \\ &= \sum_{i=1}^n |T_i^0| - |V^+ \setminus V| \\ &= \sum_{i=1}^n |T_i| \frac{|T_i^0|}{|T_i|} - |V^+ \setminus V| \\ &\geq \sum_{i=1}^n |T_i| \cdot r_k - |V^+ \setminus V| \\ &= r_k \cdot |V^+| - |V^+ \setminus V|. \end{aligned}$$

In the general case, let $W = (V^+)^-$. For every $v \in V$, all its positive neighbors are in V^+ , so $v \in (V^+)^- = W$. We conclude that $V \subseteq W$, and consequently $V^+ \subseteq W^+$. By Lemma 12, $W^+ = ((V^+)^-)^+ \subseteq V^+$, so $(W^+)^- \subseteq (V^+)^- = W$. Therefore, the special case above applies to W , and we have

$$s_k(W) \geq r_k \cdot |W^+| - |W^+ \setminus W|.$$

Since $V^+ \subseteq W^+$ and $W^+ \subseteq V^+$, we have $V^+ = W^+$. By Lemma 15, we have

$$s_k(V) \geq s_k(W) - |W \setminus V| \geq r_k \cdot |V^+| - |V^+ \setminus W| - |W \setminus V| = r_k \cdot |V^+| - |V^+ \setminus V|.$$

□

A.9 Proof of Lemma 5

This is the inverse of Lemma 12.

Lemma 16. $V \subseteq (V^+)^-$.

Proof. Choose $v \in V \subseteq V^+$. By definition of the cover $\{v\}^+ \subseteq V^+$. By the definition of the interior, we must have $v \in (V^+)^-$. □

This lemma rewrites r_k in preparation for the proof of Lemma 5.

Lemma 17. If $k > 0$, we have

$$r_k = \min_{1 \leq j \leq k} \frac{f_{d,j} - j}{f_{d,j}},$$

where $f_{d,k} = \min\{|V^+|: V \subset \mathbb{Z}^d, |V| = k\}$.

Proof. Let $k > 0$. From the definition of r_k , we have

$$\begin{aligned} r_k &= \min_{0 \leq j \leq k} \min\left\{\frac{|V^0|}{|V|} : \emptyset \neq V \subset \mathbb{Z}^d, |V^-| = j\right\} \\ &= \min_{1 \leq j \leq k} \min\left\{\frac{|V| - j}{|V|} : V \subset \mathbb{Z}^d, |V^-| = j\right\} \\ &= \min_{1 \leq j \leq k} \frac{f_{d,j} - j}{f_{d,j}}, \end{aligned}$$

where $f_{d,k} = \min\{|V|: V \subset \mathbb{Z}^d, |V^-| = k\}$. By Lemma 12, $V \supseteq (V^-)^+$. Moreover, combining Lemma 12 and Lemma 16, we have

$$V^- \subseteq ((V^-)^+)^- \subseteq V^-,$$

so $V^- = ((V^-)^+)^-$. It follows that the minimum in the definition of $f_{d,k}$ is attained when $V = (V^-)^+$. Calling $W = V^-$, we get $f_{d,k} = \min\{|W^+|: W \subset \mathbb{Z}^d, |W| = k\}$. □

We calculate $f_{d,k}$ for low d and k as a basis for induction.

Lemma 18. If $k = 0$, we have $f_{d,k} = 0$. If $d = 1$ and $k > 0$, we have $f_{d,k} = k + 1$.

Proof. We have $0 \leq f_{d,0} \leq |\emptyset^+| = 0$, so $f_{d,0} = 0$. Let $k > 0$ and $d = 1$. Let $v = \max\{v_1: v \in V\}$. Then $v + 1 \in V^+ \setminus V$. Therefore $1 + k \leq f_{d,k} \leq \{1, \dots, k\}^+ = k + 1$. So $f_{1,k} = k + 1$. □

Lemma 19. If $V \subset \mathbb{Z}^d$ and $1 \leq h \leq d$, we have $|V^+| \geq |X_h(V)^+| + \sum_{i \in D_h(V)} |S_{h,i}(V)^+|$, where

$$X_h(V) = \{v \in \mathbb{Z}^{d-1}: (v_1, \dots, v_{h-1}, i, v_{h+1}, \dots, v_d) \in V \text{ for at least one } i \in \mathbb{Z}\}$$

is the projection of V on (v_1, \dots, v_h, v_d) ,

$$D_h(V) = \{i \in \mathbb{Z}: (v_1, \dots, v_{h-1}, i, v_{h+1}, \dots, v_d) \in V \text{ for at least one } v \in \mathbb{Z}^{d-1}\}$$

is the projection of V on v_h , and

$$S_{h,i}(V) = \{v \in \mathbb{Z}^{d-1}: (v_1, \dots, v_{h-1}, i, v_{h+1}, \dots, v_d) \in V\}.$$

is the slice of V at $v_h = i$. If V is convex in the direction of the h th unit vector u , i.e. if $v \in V$ and $v + iu \in V$, with $i > 0$ implies $v + (i - 1)u \in V$, then we have $|V^+| = |X_1(V)^+| + \sum_{i \in D_1(V)} |S_{1,i}(V)^+|$.

Proof. Without loss of generality let $h = 1$. Call

$$W_0 = \{v + e : v \in V, e \in \{0\} \times \{0, 1\}^{d-1}\}$$

and

$$W_1 = \{v + e : v \in V, e \in \{1\} \times \{0, 1\}^{d-1}\} \setminus W_0.$$

Then we have $V^+ = W_0 \cup W_1$.

Let $w \in X_1(V^+)$ and $m(w) = \max\{i \in \mathbb{Z} : (i, w) \in V^+\}$. Then $(m(w), w) \notin W_0$, since otherwise $(m(w) + 1, w) \in W_1 \subseteq V^+$, which contradicts the definition of $m(w)$. Therefore $(m(w), w) \in V^+ \setminus W_0 = W_1 \setminus W_0$. Since $(m(w), w)$ is unique for w , we have $|W_1 \setminus W_0| \geq |X_1(V^+)|$. Suppose V is convex in the direction u . Choose $v \in W_1 \setminus W_0 = V^+ \setminus W_0$. Then $v = (i, w)$ for some $w \in X_1(V^+)$. Since $v \in W_1$, there is an $e \in \{0, 1\}^{d-1}$ such that $(i - 1, w + e) \in V$. Since $v \notin W_0$, we have $(i, w + e) \notin V$. Since V is convex in u , we must have that $(j, w + e) \notin V$ for all $j > i$, so $i = \max\{j \in \mathbb{Z} : (j, w + e) \in V\}$ is unique. Therefore, $|W_1 \setminus W_0| \leq |X_1(V^+)|$. We have $|W_1 \setminus W_0| = |X_1(V^+)|$ if V is convex in the direction u , and $|W_1 \setminus W_0| \geq |X_1(V^+)|$ in general.

We will now show that $X_1(V^+) = X_1(V)^+$. We have that $v \in X_1(V)^+$ if and only if there exists $e \in \{0, 1\}^{d-1}$ such that $v - e \in X_1(V)$. This happens if and only if there exist $e \in \{0, 1\}^{d-1}$ and $i \in \mathbb{Z}$ such that $(i, v - e) \in V$, which is equivalent to the existence of $i \in \mathbb{Z}$ such that $(i, v) \in V^+$, which happens if and only if $v \in X_1(V^+)$. Therefore $X_1(V)^+ = X_1(V^+)$, and we have $|W_1 \setminus W_0| \geq |X_1(V)^+|$, with equality if V is convex in the direction u .

Choose $i \in D_1(V)$. We have that $v \in S_{1,i}(V)^+$ happens if and only if there exists $e \in \{0, 1\}^{d-1}$ such that $v - e \in S_{1,i}(V)$, equivalently $(i, v - e) \in V$, which happens if and only if $(i, v) \in W_0$, or $v \in S_{1,i}(W_0)$. It follows that $|S_{1,i}(V)^+| = |S_{1,i}(W_0)|$.

We have

$$V^+ = (W_1 \setminus W_0) \cup W_0 = (W_1 \setminus W_0) \cup \bigcup_{i \in D(V)} \{v \in W_0 : v_1 = i\}.$$

Since all these sets are disjoint, we have

$$|V^+| = |W_1 \setminus W_0| + \sum_{i \in D_1(V)} |S_{1,i}(W_0)| \geq |X_1(V)^+| + \sum_{i \in D_1(V)} |S_{1,i}(V)^+|,$$

with equality if V is convex in u . □

The next lemma states that $b_{d,k}$ is the largest number of the form $q^{d-l}q^l$ that does not exceed k .

Lemma 20. *We have $0 \leq k - b_{d,k} < \frac{b_{d,k}}{\lfloor k^{1/d} \rfloor}$.*

Proof. Write $q = \lfloor k^{1/d} \rfloor$. Then $q^{d-l}(q+1)^l \leq k$ is equivalent to

$$(d-l) \log(q) + l \log(q+1) \leq \log(k),$$

and to

$$l \leq \frac{\log(k) - d \log(q)}{\log(q+1) - \log(q)} = l_{d,k},$$

where $l_{d,k}$ is defined in Lemma 5. It follows that $b_{d,k} = q^{d-l_{d,k}}(q+1)^{l_{d,k}} \leq k$, but

$$b_{d,k} \frac{\lfloor k^{1/d} \rfloor + 1}{\lfloor k^{1/d} \rfloor} = q^{d-l_{d,k}-1}(q+1)^{l_{d,k}+1} > k.$$

□

Lemma 21. Let $c_{d,k} = b_{d,k} - b_{d,k-1}$ and $c_{d,k}^+ = b_{d,k}^+ - b_{d,k-1}^+$ if $k > 0$ and $c_{d,k} = b_{d,k} = 1$ and $c_{d,k}^+ = b_{d,k}^+ = 2^d$ if $k = 1$. If $k \neq b_{d,k}$, then $c_{d,k} = c_{d,k}^+ = 0$. If $k = b_{d,k}$, then

$$c_{d,k} = k/(q'_{d,k} + 1),$$

where $q'_{d,k} = \lfloor k^{1/d} \rfloor$ and $l'_{d,k} = l_{d,k}$ if $l_{d,k} > 0$ and $q'_{d,k} = \lfloor k^{1/d} \rfloor - 1$ and $l'_{d,k} = d$ if $l_{d,k} = 0$. If $0 < k = b_{d,k}$ and $d > 1$, then

$$c_{d,k}^+ = f_{d-1, c_{d,k}}.$$

If $k = 1$ and $d > 1$ we have $c_{d,1}^+ = 2^d > f_{d-1, c_{d,1}} = f_{d-1, 1} = 2^{d-1}$.

Proof. The part for $k \neq b_{d,k}$ follows immediately from the definition of $b_{d,k}$. Let $k = b_{d,k}$. We have

$$b_{d,k} = (q'_{d,k})^{d-l'_{d,k}} (q'_{d,k} + 1)^{l'_{d,k}},$$

and

$$b_{d,k-1} = (q'_{d,k})^{d-l'_{d,k}+1} (q'_{d,k} + 1)^{l'_{d,k}-1}.$$

Therefore, if $k > 1$,

$$c_{d,k} = (q'_{d,k})^{d-l'_{d,k}} (q'_{d,k} + 1)^{l'_{d,k}-1} (q'_{d,k} + 1 - q'_{d,k}) = (q'_{d,k})^{d-l'_{d,k}} (q'_{d,k} + 1)^{l'_{d,k}-1} = b_{d,k}/(q'_{d,k} + 1).$$

If $k = 1$, we have $l_{d,k} = 0$, so $l'_{d,k} = d$ and $q'_{d,k} = 0$, so the equality still holds. Completely analogously, we get

$$c_{d,k}^+ = (q'_{d,k} + 1)^{d-l'_{d,k}} (q'_{d,k} + 2)^{l'_{d,k}-1} = f_{d-1, c_{d,k}},$$

where the latter equality is meaningful only if $d > 1$. The inequality for $k = 1$ is trivial. \square

Lemma 22. The following two statements hold:

1. $f_{d,m} \leq f_{d,k} + f_{d,l}$, where $m = k + l$;
2. If $m \geq \max(n, k, l)$, $m \in B_d$, and $m + n = k + l$, then $f_{d,m} + f_{d,n} \leq f_{d,k} + f_{d,l}$.

Proof. We use induction on d and k (downward). If $d = 1$ both statements are easily checked from Lemma 18. If $k = m$ both are trivial. Fix m and n . Suppose that both statements hold for all m, n, k, l in smaller dimensions, and for all larger values of $k \leq m$.

Without loss of generality, assume $k \geq l$. We consider

$$f_{d,k} + f_{d,l} = b_{d,k}^+ + f_{d-1, k-b_{d,k}} + b_{d,l}^+ + f_{d-1, l-b_{d,l}}.$$

Let $k' = \min\{i \in B_d : i > k\}$. One of the cases holds:

1. $l - d_{b,l} > 0$ and $l - d_{b,l} + k - b_{d,k} < c_{d,k'}$;
2. $l - d_{b,l} > 0$ and $l - d_{b,l} + k - b_{d,k} \geq c_{d,k'}$;
3. $l - d_{b,l} = 0$ and $l - d_{b,l} + c_{d,b_{d,l}} < c_{d,k'}$;
4. $l - d_{b,l} = 0$ and $l - d_{b,l} + c_{d,b_{d,l}} \geq c_{d,k'}$.

In Case 1, we use induction on d for Statement 1 and write

$$f_{d,k} + f_{d,l} \geq b_{d,k}^+ + f_{d-1, l-d_{b,l}+k-b_{d,k}} + b_{d,l}^+ f_{d-1, c_{d,i}} = f_{d, k+l-d_{b,l}} + f_{d, b_{d,l}}.$$

In Case 2, we note that $l - b_{d,l} < c_{d,b_{d,l}} \leq c_{d,k'}$, and use induction on d for Statement 2, and Lemma 21, to write

$$f_{d,k} + f_{d,l} \geq b_{d,k}^+ + f_{d-1,c_{d,k'}} + b_{d,l}^+ + f_{d-1,l-d_{b,l}+k-b_{d,k}-c_{d,k'}} = f_{d,k'} + f_{d,l+k-k'}.$$

In Case 3 and 4, we note that $l = b_{d,l}$ and write, using Lemma 21,

$$f_{d,k} + f_{d,l} \geq b_{d,k}^+ + f_{d-1,k-b_{d,k}} + b_{d,l-c_{d,l}}^+ + f_{d-1,c_{d,l}},$$

where we write \geq to cover the case that $l = 1$. In Case 3 we use induction on d for Statement 1 and write

$$f_{d,k} + f_{d,l} \geq b_{d,k}^+ + f_{d-1,k-b_{d,k}+c_{d,b_{d,l}}} + b_{d,l-c_{d,l}}^+ = f_{d,k+c_{d,l}} + f_{d,l-c_{d,l}}.$$

In Case 4, since $c_{d,l} \leq c_{d,k'}$, we use induction on d for Statement 2, and Lemma 21, to write

$$f_{d,k} + f_{d,l} \geq b_{d,k}^+ + f_{d-1,c_{d,k'}} + b_{d,l-c_{d,l}}^+ + f_{d-1,c_{d,l}+k-b_{d,k}-c_{d,k'}} = f_{d,k'} + f_{d,l+k-k'}.$$

In all cases, we have $f_{d,k} + f_{d,l} \geq f_{d,k''} + f_{d,l''}$ with $k'' > k$ and $k'' + l'' = k + l$. By the induction hypotheses on k we have

$$f_{d,k} + f_{d,l} \geq f_{d,k''} + f_{d,l''} \geq f_{d,m}.$$

Since $k'' \leq k' \leq m$, we retain the conditions of Statement 2, so we can also call on the induction hypothesis for k in Statement 2, obtaining

$$f_{d,k} + f_{d,l} \geq f_{d,k''} + f_{d,l''} \geq f_{d,m} + f_{d,n},$$

and we have proved both statements. \square

Lemma 23. *For every $d > 0$ and $k \geq 0$ there exists $F_{d,k} \subset \mathbb{Z}^d$ such that $|F_{d,k}| = k$ and $|F_{d,k}^+| = f_{d,k}$. Moreover, if $k \leq k'$, then $F_{d,k} \subseteq F_{d,k'}$.*

Proof. We use induction on d . For $d = 1$, $F_{d,k} = \{1, \dots, k\}$ satisfies $|F_{d,k}| = k$ and $|F_{d,k}^+| = k + 1 = f_{d,k}$ by Lemma 18. It is immediate that $F_{d,k} \subseteq F_{d,k'}$ if $k \leq k'$.

Suppose the Lemma holds for all smaller values of d . Define

$$B_{d,k} = \{v \in \mathbb{Z}^d : 1 \leq v_i \leq \lfloor k^{1/d} \rfloor + 1 \text{ for } 1 \leq i \leq l_{d,k}, \text{ and } 1 \leq v_i \leq \lfloor k^{1/d} \rfloor \text{ for } l_{d,k} < i \leq d\},$$

and

$$F_{d,k} = B_{d,k} \cup \{(w_1, \dots, w_{l_{d,k}}, \lfloor k^{1/d} \rfloor + 1, w_{l_{d,k}+1}, \dots, w_{d-1}) : w \in F_{d-1,k-b_{d,k}}\}.$$

Clearly, $|B_{d,k}| = b_{d,k}$ and $B_{d,k}^+ = b_{d,k}^+$. We have $|F_{d,k}| = b_{d,k} + (k - b_{d,k}) = k$. Since

$$b - b_{d,k} < b_{d,k} / \lfloor k^{1/d} \rfloor = q_{d,k}^{d-l_{d,k}-1} (q_{d,k} + 1)^{l_{d,k}},$$

by Lemma 20, we have

$$\begin{aligned} F_{d-1,b_{d,k}} &\subset F_{d-1,b_{d,k}/\lfloor k^{1/d} \rfloor} \\ &= B_{d-1,b_{d,k}/\lfloor k^{1/d} \rfloor} \\ &= \{v \in \mathbb{Z}^{d-1} : 1 \leq v_i \leq \lfloor k^{1/d} \rfloor + 1 \text{ for } 1 \leq i \leq l_{d,k}, \text{ and } 1 \leq v_i \leq \lfloor k^{1/d} \rfloor \text{ for } l_{d,k} < i \leq d-1\} \\ &= X_{l_{d,k}+1}(B_{d,k}). \end{aligned}$$

Therefore, by the induction hypothesis and Lemma 19 we have $|F_{d,k}^+| = b_{d,k}^+ + f_{d-1,k-b_{d,k}} = f_{d,k}$.

To show the inclusion it suffices to take $k' = k + 1$. If $b_{d,k} < b_{d,k+1}$, then $F_{d,k+1} = B_{d,k+1} \supset B_{d,k}$, and $|B_{d,k+1} \setminus B_{d,k}| = k + 1 - b_{d,k}$ by Lemma 21. We have

$$\begin{aligned} F_{d,k+1} \setminus B_{d,k} &= \{(w_1, \dots, w_{l_{d,k}}, \lfloor k^{1/d} \rfloor + 1, w_{l_{d,k}+1}, \dots, w_{d-1}) : w \in B_{d-1, k+1-b_{d,k}}\} \\ &= \{(w_1, \dots, w_{l_{d,k}}, \lfloor k^{1/d} \rfloor + 1, w_{l_{d,k}+1}, \dots, w_{d-1}) : w \in F_{d-1, k+1-b_{d,k}}\}. \end{aligned}$$

The same holds immediately from the definition if $b_{d,k} = b_{d,k+1}$. The result that $F_{d,k} \subset F_{d,k+1}$ now follows from the induction hypothesis. \square

Lemma 24. *Let $d > 1$, and suppose we have $k_1, \dots, k_m \geq 0$ with $k_0 = \max_{1 \leq i \leq m} k_i$. Then there exists $V \subset \mathbb{Z}^d$ such that $|V| = \sum_{i=1}^m k_i$ and $|V^+| = \sum_{i=0}^m f_{d-1, k_i}$.*

Proof. Without loss of generality, assume $k_1 \geq \dots \geq k_m$. For $i = 1, \dots, m$, let $V_i = \{(i, v) : v \in F_{d-1, k_i}\}$, where $F_{d,k}$ is defined in Lemma 23, and let $V = \bigcup_{i=1}^m V_i$. Then $|V| = \sum_{i=1}^m k_i$ by Lemma 23. Moreover, since $F_{d-1, k_i} \subseteq F_{d-1, k_1}$ for $1 \leq i \leq m$, we have $X_1(V) = V_1$, and V is convex in $(1, 0, \dots, 0)$. By Lemma 19 and Lemma 23,

$$|V^+| = |X_1(V)| + \sum_{i=1}^m |F_{d-1, k_i}| = \sum_{i=0}^m f_{d-1, k_i}.$$

\square

Lemma 25. *We have $g_{d,k} = \min\{|V^+| : V \subset \mathbb{Z}^d, |V| = k\} = f_{d,k}$.*

Proof. We use induction. If $k = 0$, we have $0 \leq g_{d,0} \leq |\emptyset^+| = 0$, so $g_{d,0} = 0 = f_{d,0}$. Let $k > 0$ and $d = 1$. Let $v = \max\{v_1 : v \in V\}$. Then $v + 1 \in V^+ \setminus V$. Therefore $1 + k \leq g_{d,k} \leq \{1, \dots, k\}^+ = k + 1$. If $d = 1$, we have $l_{d,k} = 0$, so $f_{1,k} = k + 1 = g_{1,k}$.

Choose k, d and assume the statement of the Lemma holds for all lower values of d and k .

Let V be such that $|V| = k$. For $1 \leq i \leq d$, let

$$m_i = \{j \in \mathbf{Z} : v_i = j \text{ for some } v \in V\},$$

the number of coordinates in dimension v_i that V uses. Remark that if $\max_{1 \leq i \leq d} m_i \geq q$, where $q = \lfloor k^{1/d} \rfloor$, or otherwise

$$|V| \leq \prod_{i=1}^d m_i \leq (\max_{1 \leq i \leq d} m_i)^d < q^d \leq k.$$

If $\max_{1 \leq i \leq d} m_i = k^{1/d}$, then V must be a d -cube of dimension $k^{1/d}$. Then $|V^+| = (k^{1/d} + 1)^d = b_{d,k}^+ = f_{d,k}$, and the result of the lemma follows immediately. In the rest of the proof, we can therefore assume that $\max_{1 \leq i \leq d} m_i > q$

Remark also that $|V^+|$ is invariant by definition to a permutation of the dimensions, so without loss of generality we can assume that $m = m_1 \geq q + 1$.

By Lemma 19 and the induction hypothesis on d we have

$$|V^+| \geq |X_1(V)^+| + \sum_{i=1}^m |S_{1,i}(V)^+| \geq \sum_{i=0}^m f_{d-1, n_i},$$

where $n_0 = |X_1(V)|$ and $n_i = |S_{1,i}(V)^+|$. Without loss of generality, let $n = n_m = \min_{1 \leq i \leq d} n_i$. We have

$$k = |V| = \sum_{i=1}^m n_i \geq mn \geq (q + 1)n,$$

so $n \leq k/(q + 1)$.

By Lemma 24 there exists a W such that $|W| = \sum_{i=1}^{m-1} n_i$ and $|W^+| = \sum_{i=0}^{m-1} f_{d-1, n_i}$. By the induction hypothesis on k we have

$$|V^+| \geq |W^+| + f_{d-1, n} \geq f_{d, k-n} + f_{d-1, n} = b_{d, k-n}^+ + f_{d-1, k-n-b_{d, k-n}} + f_{d-1, n}.$$

If $b_{d, k-n} = b_{d, k}$, we have, by Lemma 22,

$$|V^+| \geq b_{d, k}^+ + f_{d-1, k-n-b_{d, k}} + f_{d-1, n} \geq b_{d, k}^+ + f_{d-1, k-b_{d, k}} = f_{d, k}.$$

Suppose $b_{d, k-n} < b_{d, k}$. Then, by Lemma 21,

$$k - n \geq b_{d, k} - b_{d, k}/(q + 1) \geq b_{d, k} - b_{d, k}/(q' + 1) = b_{d, k} - c_{d, k} = b_{d, k-1},$$

so $b_{d, k-n} \geq b_{d, k} - c_{d, k}$. Then $k - n < b_{d, k}$, so that, also by Lemma 21,

$$k - n - b_{d, k-n} < b_{d, k} - (b_{d, k} - c_{d, k}) = c_{d, k}.$$

Moreover, $n \leq k/(q + 1) \leq k/(q' + 1) = c_{d, k}$, by Lemma 21, where $q' = q'_{d, k}$ and $c_{d, k}$ are defined in that lemma. Finally, $k - b_{d, k-n} - c_{d, k} = k - b_{d, k} < c_{d, k}$ by definition of $b_{d, k}$. By Lemma 22 and Lemma 21, we have

$$|V^+| \geq b_{d, k-n}^+ + f_{d-1, c_{d, k}} + f_{d-1, k-c_{d, k}-b_{d, k-n}} = b_{d, k}^+ + f_{d-1, k-b_{d, k}} = f_{d, k}.$$

Since $|V^+| \geq f + d, k$ holds for all $V \subseteq \mathbb{Z}^d$ with $|V| = k$, it follows that $g_{d, k} \geq f_{d, k}$.

By Lemma 23 there exists a $W \subseteq \mathbb{Z}^d$ such that $|W| = k$ and

$$|W^+| = f_{d, k} = b_{d, k}^+ + f_{d-1, k-b_{d, k}} = (q + 1)(b_{d-1, b_{d, k}/q}) + f_{d-1, k-b_{d, k}},$$

so $g_{d, k} \leq f_{d, k}$. Combining, we have $g_{d, k} = f_{d, k}$, as desired. \square

Lemma 5. *If $k = 0$, we have $r_k = 1$. If $k > 0$, we have*

$$r_k = \min_{1 \leq j \leq k} \frac{f_{d, j} - j}{f_{d, j}},$$

where, $f_{1, k} = (k + 1)\mathbb{1}\{k > 0\}$ and, for $d > 1$, we have recursively

$$f_{d, k} = b_{d, k}^+ + f_{d-1, k-b_{d, k}}.$$

Here,

$$b_{d, k} = (\lfloor k^{1/d} \rfloor)^{d-l_{d, k}} (\lfloor k^{1/d} \rfloor + 1)^{l_{d, k}},$$

and

$$b_{d, k}^+ = (\lfloor k^{1/d} \rfloor + 1)^{d-l_{d, k}} (\lfloor k^{1/d} \rfloor + 2)^{l_{d, k}},$$

where

$$l_{d, k} = \left\lfloor \frac{\log(k) - d \log(\lfloor k^{1/d} \rfloor)}{\log(\lfloor k^{1/d} \rfloor + 1) - \log(\lfloor k^{1/d} \rfloor)} \right\rfloor.$$

Proof. Combine Lemma 17 with Lemma 25. \square

A.10 Proof of Lemma 6

The following lemma generalizes Lemma 12.

Lemma 26. $V^{(i)} \subseteq V$.

Proof. Let $W = ((V^-)^\cdots)^-$, where the interior operation $(\cdot)^-$ is done i times. Choose $v \in V^{(i)}$. By definition of the cover there must be a $w \in W$ such that $v = w + e$ with $e \in \{0, \dots, i\}^d$. By definition of the interior, $w \in W$ implies that every $u = w + e$ with $e \in \{0, \dots, i\}^d \in V$, so in particular $v \in V$. \square

Lemma 6. *If $i \geq \lfloor |V|^{1/d} \rfloor$, then $V^{(i)} = \emptyset$.*

Proof. Let $W = ((V^-)^\cdots)^-$, where the interior operation $(\cdot)^-$ is done i times. If $W = \emptyset$, then $V^{(i)} = \emptyset$ and we are done. We will assume that $W \neq \emptyset$ and arrive at a contradiction. Let $w \in W$. Then $w + e \in V^{(i)}$ for all $e \in \{0, \dots, i\}^d$. Therefore $|V^{(i)}| \geq (i+1)^d > (|V|^{1/d})^d = |V|$, which contradicts Lemma 26. \square

A.11 Proof of Theorem 5

We first prove the relevant bound for $s_k(V)$.

Lemma 27. $\check{s}_k(V) \leq s_k(V)$

Proof. If $\chi_V > k$, then $s_k(V) > 0$, as follows immediately from the definition of $s_k(V)$, so

$$\mathbb{1}\{\chi_V > k\} \leq s_k(V).$$

For any $i \geq 0$, by Lemma 26, $V^{(i)} \subseteq C$. Therefore, by Theorem 4 and Lemma 9,

$$\underline{s}_k(V^{(i)}) \leq s_k(V^{(i)}) = \min\{|R|: \chi_{V^{(i)} \setminus R} \leq k\} \leq \min\{|R|: \chi_{V \setminus R} \leq k\} \leq s_k(V)$$

Since $\mathbb{1}\{\chi_V > k\}$ and $\underline{s}_k(V^{(i)})$ for $i = 0, \dots, |V|^{1/d}$ are all smaller than $s_k(V)$, so is their maximum. Since $s_k(V)$ is an integer, the result follows. \square

Theorem 5. *For every $V \subseteq M$, let*

$$\underline{\mathbf{a}}(V) = \sum_{i=1}^n \check{s}_{k_M}(\mathbf{C}_i),$$

where $\mathbf{C}_1, \dots, \mathbf{C}_n$ are disconnected clusters such that $\mathbf{C}_1 \cup \dots \cup \mathbf{C}_n = V \cap \mathbf{Z}$. Then, for all $P \in \Omega$,

$$P(\underline{\mathbf{a}}(V) \leq a_P(V) \text{ for all } V \subseteq M) \geq 1 - \alpha.$$

Proof. By Lemma 27, Lemma 2, and Theorem 1, we have

$$\underline{\mathbf{a}}(V) \leq \sum_{i=1}^n s_{k_M}(\mathbf{C}_i) = s_{k_M}(\mathbf{C}_1 \cup \dots \cup \mathbf{C}_n) = s_{k_M}(V \cap \mathbf{Z}) = \check{\mathbf{a}}(V).$$

By Theorem 1, we therefore have, for all $P \in \Omega$,

$$P(\underline{\mathbf{a}}(V) \leq a_P(V) \text{ for all } V \subseteq M) \leq P(\check{\mathbf{a}}(V) \leq a_P(V) \text{ for all } V \subseteq M) \geq 1 - \alpha.$$

\square

A.12 Proof of Lemma 7

Lemma 7. *Let $k = n^d$ and c be a vector of d positive integers. If the dimensions of a hyperrectangle R are $(n+1)c_i - 1$ for $i = 1, \dots, d$, then the bound of Theorem 4 is exact, so that the optimal k -separator of R has $|R| - n^d \Pi c_i$ voxels.*

Proof. We first infer a k -separator K of the size $|R| - n^d \Pi c_i$. Assume, the $\min(R) = 1$ (as a vector). A voxel is an element of K if and only if there are i and $j \in \{1, 2, \dots, c_i - 1\}$ such that the i -th coordinate of the voxel is equal to $(n+1)j$. Then, $R \setminus K$ consists of Πc_i separated d -cubes of the size $k = n^d$. Thus, K is a k -separator of R . This completes the first part of the proof.

Next, we show that the separator is optimal. It follows from Lemma 5, that in our setting when $k = n^d$, $l_{d,k} = 0$ and $f(d, k) = (n+1)^d$. Moreover, it follows from the definition of r_k in Lemma 5 that $\frac{f_{d,j}-j}{f_{d,j}}$ is minimal when $j = k$. Thus, $r_k = r_{n^d} = \frac{(n+1)^d - n^d}{(n+1)^d}$. To complete the proof, it is sufficient to show that

$$\frac{(n+1)^d - n^d}{(n+1)^d} |R^+| - |R^+ \setminus R| = |R| - n^d \Pi c_i.$$

The left-hand side of the above equation is the lower bound from Theorem 4, while the right hand side is the size our separator set. The rest follows by easy transformations, by applying $|R^+| = \Pi(n+1)c_i = (n+1)^d \Pi c_i$ and $|R^+ \setminus R| = |R^+| - |R|$.

Since the lower bound is reached, the k -separator K is optimal. This completes the proof. \square

A.13 Proof of Theorem 6

Theorem 6. *If $k_M = 0$, then for all $V \subseteq M$ we have*

$$\underline{\mathbf{a}}(V) = \check{\mathbf{a}}(V) = \mathbf{a}(V) = |V \cap \mathbf{Z}|.$$

Proof. We will first show that $\mathbf{a}(V) = \check{\mathbf{a}}(V)$, then that $\check{\mathbf{a}}(V) = |V \cap \mathbf{Z}|$ and $\underline{\mathbf{a}}(V) = |V \cap \mathbf{Z}|$.

From (4) we have, for all $V \subseteq M$,

$$\phi_V = \mathbb{1}\{\chi_{V \cap \mathbf{Z}} > 0\} = \mathbb{1}\{|V \cap \mathbf{Z}| > 0\}.$$

Therefore, $\phi_V \leq \phi_W$ if $V \subseteq W$, and we have, for all $V \subseteq M$,

$$\psi_V = \min\{\phi_W : V \subseteq W \subseteq M\} = \phi_V.$$

Therefore, for all $V \subseteq M$, $\underline{\psi}_V = \mathbb{1}\{\chi_{V \cap \mathbf{Z}} > 0\} = \psi_V$, so that $\mathbf{a}(V) = \check{\mathbf{a}}(V)$.

Now by Theorem 1 we have $\check{\mathbf{a}}(V) = s_0(V \cap \mathbf{Z})$, and for any $W \subseteq M$, $s_0(W) = \min\{|R| : \chi_{W \setminus R} = 0\} = |W|$, so $\check{\mathbf{a}}(V) = |V \cap \mathbf{Z}|$.

If $k = 0$, then $r_k = 1$ by definition of r_k , so $\underline{s}_0(V) = |V^+| - |V^+ \setminus V| = |V|$. It follows from Theorem 5 that, if $\mathbf{C}_1, \dots, \mathbf{C}_n$ are defined as in that theorem, then

$$\underline{\mathbf{a}}(V) \geq \sum_{i=1}^n \underline{s}_0(\mathbf{C}_i) = \sum_{i=1}^n |\mathbf{C}_i| = |V \cap \mathbf{Z}|.$$

We have, for all $V \subseteq M$,

$$|V \cap \mathbf{Z}| \leq \underline{\mathbf{a}}(V) \leq \mathbf{a}(V) = \check{\mathbf{a}}(V) = |V \cap \mathbf{Z}|,$$

so we must have equality and the statement of the theorem follows. \square

A.14 Proof of Theorem 7

We first prove an upper bound on $\underline{s}_k(V)$.

Lemma 28. *We have*

$$\underline{s}_k(V) \leq \frac{r_k - r_{|V|}}{1 - r_{|V|}} \cdot |V|.$$

Proof. If $k = 0$, we have $r_k = 1$, so the statement of the Lemma reads $\underline{s}_k(V) \leq |V|$, which follows immediately from the definition. Let $k > 0$. We have

$$\begin{aligned} \underline{s}_k(V) &= r_k \cdot |V^+| - |V^+ \setminus V| \\ &= r_k \cdot |V^+| - |V^+| + |V| \\ &= |V| - (1 - r_k) \cdot |V^+| \\ &\leq |V| - (1 - r_k) \min\{|W^+| : W \subseteq \mathbb{Z}^d, |W| = |V|\} \\ &= |V| - (1 - r_k) f_{|V|}, \end{aligned}$$

where $f_k = f_{d,k}$ is defined in Lemma 5, and we suppress the dependence on d here. We have

$$f_k = \frac{k}{1 - \frac{f_k - k}{f_k}} \geq \frac{k}{1 - \min_{1 \leq j \leq k} \frac{f_j - j}{f_j}} = \frac{k}{1 - r_k},$$

so that

$$\underline{s}_k(V) \leq \left(1 - \frac{1 - r_k}{1 - r_{|V|}}\right) \cdot |V|,$$

which rewrites to the statement of the Lemma. \square

Theorem 7. *For every cluster $\mathbf{C} \subseteq \mathbf{Z}$, we have*

$$\underline{\mathbf{a}}(\mathbf{C}) \leq \left\lceil \frac{r_k - r_{|\mathbf{C}|}}{1 - r_{|\mathbf{C}|}} \cdot |\mathbf{C}| \right\rceil \vee \mathbf{1}\{|\mathbf{C}| > k\}.$$

Proof. Choose any $i \geq 0$. By lemma 26, $V^{(i)} \subseteq V$. By Lemma 28, we have, since r_k is decreasing in k by definition,

$$\underline{s}_k(V^{(i)}) \leq \left(1 - \frac{1 - r_k}{1 - r_{|V^{(i)}|}}\right) \cdot |V^{(i)}| \leq \left(1 - \frac{1 - r_k}{1 - r_{|V|}}\right) \cdot |V|.$$

Therefore

$$\check{s}_k(V) \leq \left\lceil \left(1 - \frac{1 - r_k}{1 - r_{|V|}}\right) \cdot |V| \right\rceil \vee \mathbf{1}\{\chi_V > k\}.$$

The result of the Proposition now follows directly from Theorem 5, remarking that if \mathbf{C} is a cluster, that $\mathbf{1}\{\chi_{\mathbf{C}} > k\} = \mathbf{1}\{|\mathbf{C}| > k\}$. \square

A.15 Proof of Lemma 8

Lemma 8. *We have $s_k(V) \leq \tilde{r}_k \cdot |V|$, where $\tilde{r}_k = (b_{d,k}^+ - b_{d,k})/b_{d,k}^+$.*

Proof. By definition of $b_{d,k}^+$ and $b_{d,k}$ there are integers q_1, \dots, q_d such that $b_{d,k} = q_1 q_2 \cdots q_d \leq k$ and $b_{d,k}^+ = (q_1 + 1)(q_2 + 1) \cdots (q_d + 1)$. Let $R'_1 \subseteq \mathbb{Z}^d$ be the set for which the i th coordinate is divisible by $q_i + 1$, for $i = 1, \dots, d$. Then R'_1 is a k -separator of \mathbb{Z}^d , so that $R_1 = R'_1 \cap V$ is a k -separator of V . Let $R'_2, \dots, R'_{b^+ - d, k}$ be analogously defined as all translations of R'_1 by $\{0, \dots, q_1\} \times \cdots \times \{0, \dots, q_d\}$, and define $R_2, \dots, R_{b^+ - d, k}$ analogously.

For every $v \in V$, there are exactly $b_{d,k}^+ - b_{d,k}$ sets $i \in \{1 \text{ dots } b_{d,k}^+\}$ for which $v \in R'_i$, so $v \in R_i$ and $b_{d,k}$ for which it is in $\mathbb{Z}^d \setminus R'_i$, so $v \in V \setminus R_i$. We have

$$\sum_{i=1}^{b_{d,k}^+} |R_i| = (b_{d,k}^+ - b_{d,k}) \cdot |V|.$$

It follows that there exists an R_i for which $|R_i| \leq (b_{d,k}^+ - b_{d,k})/b_{d,k}^+ \cdot |V|$. Since R_i is a k -separator of V , we have $s_k(V) \leq \tilde{r}_k \cdot |V|$. \square

A.16 Proof of Theorem 8

We prove a slightly tighter bound in Lemma 29. We first define this bound. Let $\mathbf{Z} \cap M = \mathbf{C}_1 \cup \dots \cup \mathbf{C}_n$, where $\mathbf{C}_1, \dots, \mathbf{C}_n$ are disconnected clusters. Let $J_0 = \emptyset$, and for $j = 1, 2, \dots$, let

$$J_{j+1} = \{1 \leq i \leq n : |\mathbf{C}_i| > k_{M \setminus \mathbf{D}_j}\},$$

and $\mathbf{D}_i = \bigcup_{j \in J_i} \mathbf{C}_j$. Define $\mathbf{D} = \lim_{i \rightarrow \infty} \mathbf{D}_i$. To obtain \mathbf{D} , therefore, we find all significant clusters according to classical cluster-extent thresholding, update the cluster extent threshold by removing those clusters from the mask, and iterate. This procedure does not have the TDP guarantee (7) unless $k_M = 0$. Lemma 29 says that the closed testing procedure is at most as powerful as this anti-conservative procedure.

Lemma 29. *Let $\bar{\mathbf{a}}(V) = s_{k_{M \setminus \mathbf{D}}}(V \cap \mathbf{Z})$, then, for every $V \subseteq M$,*

$$\mathbf{a}(V) \leq \bar{\mathbf{a}}(V).$$

Proof. Choose any $V \subseteq M$. Define $\bar{\psi}_V = \mathbb{1}\{\chi_{V \cap \mathbf{Z}} > k_{M \setminus \mathbf{D}}\}$. We will show that $\bar{\psi}_V \geq \psi_V$ by contradiction. Suppose that $\bar{\psi}_V = 0$ and $\psi_V = 1$. Define $\mathbf{W} = V \cup (M \setminus \mathbf{D})$. Since $W \supseteq V$ and $\psi_V = 1$, we have $\chi_{W \cap \mathbf{Z}} > k_W \geq k_{M \setminus \mathbf{D}}$. The largest cluster in $W \cap \mathbf{Z}$ is therefore a subset of a cluster of $M \cap \mathbf{Z}$ of size at least $k_{M \setminus \mathbf{D}}$. All such clusters are in fully contained in \mathbf{D} by definition of \mathbf{D} . Therefore, the largest cluster of $W \cap \mathbf{Z}$ is also a cluster of $V \cap \mathbf{Z}$. Therefore, since $\bar{\psi}_V = 0$,

$$\chi_{W \cap \mathbf{Z}} \leq \chi_{V \cap \mathbf{Z}} \leq k_{M \setminus \mathbf{D}} \leq k_{V \cup (M \setminus \mathbf{D})} = k_W,$$

whence $\psi_V = 0$ since $V \subseteq W \subseteq M$, and we have a contradiction.

Starting from $\bar{\psi}_V \geq \psi_V$, the rest of the proof is completely analogous to the proof of Theorem 1. \square

Theorem 8. *Let $\bar{\mathbf{a}}(V) = s_{k_{M \setminus \mathbf{Z}}}(V \cap \mathbf{Z})$, then, for every $V \subseteq M$,*

$$\mathbf{a}(V) \leq \bar{\mathbf{a}}(V).$$

Proof. This is an immediate consequence of Lemma 29 if we remark that $\mathbf{D} \subseteq \mathbf{Z}$, so $k_{M \setminus \mathbf{D}} \geq k_{M \setminus \mathbf{Z}}$. \square

B Heuristic algorithms to minimize k -separators: pseudocode

In this section we give the pseudocode of the algorithms described in Section 5.7.

B.1 Sampling algorithm to minimize separator sets.

Algorithm 1: Initial clustering generator: phase 1

Input: A set of voxels V , the number of runs r , the number of candidate clusters s , allowed missing voxels a , allowed missing voxels step A .

Output: a clustering Z of V

function gencandidatecluster (Z)

```

  for ( $l := k; l \geq k - a; l := l - A$ )
     $C := \{v\}$ , where  $v$  is free random (i.e., non-cluster or non-separator) voxel
    while there is a free  $w$  adjacent to a voxel in  $C$  and  $|C| < l$  do  $C := C \cup \{w\}$ 
  return the candidate cluster  $C$  that minimizes the separator size of  $Z \cup \{C\}$ 

```

// Main procedure starts here.

repeat r times

```

   $Z := \emptyset$ 
  while there is a free voxel that is not adjacent to a cluster do
    Infer  $s$  candidate clusters by gencandidatecluster ( $Z$ )
     $Z := Z \cup \{C^*\}$ , where  $C^*$  is the candidate that minimizes the separator size.
  return the clustering  $Z$  with minimal separator set.

```

Algorithm 2: Local optimization: phase 2

Input: A clustering Z of a voxel set V with a separator set X , the number of big runs E , the number of searches in a fixed subgraph e , the number of neighbouring clusters M , and time limit threshold T

Output: A clustering Z of V with a separator set smaller than $|X|$ (if found)

repeat until time limit T is not reached or E times

```

  Take  $G \subset Q$  from a connected component  $Q$  of the whole voxel graph  $V$  such that there is a set  $A$  of at most  $M$  adjacent clusters such that  $G$  contains every voxel whose neighbours are only in  $X \cup \cup A$ . repeat
  | Clear the voxels from  $G$ 
  | Run phase I with  $r = 1$  to fill the clustering and update  $Z$  if the score is improved
  until there is no improvement in the last  $e$  steps

```

The algorithm consists of two phases: inferring an initial clustering, and improving regions consisting of a small number of neighbouring clusters. In the first phase, the algorithm starts from an empty clustering. It generates s candidate clusters, where s is a small integer, usually between 1 and 10. Each candidate cluster is created starting from a randomly chosen available voxel by a sequence of insertions of adjacent voxels such that the induced size of its separator is kept small. Then, the best candidate cluster, i.e., the cluster with the separator's minimal size, is inserted into the current clustering. The procedure is repeated until there is no space to insert a new cluster. The second phase consists of repetitions of local improvements. The algorithm randomly takes a small number of neighbouring clusters, removes them from the current clustering, and applies a procedure similar to the first phase to find a better setting of clusters. In testing, we used the following sets of parameters:

- For the initial clustering in phase I: $r = 1000$, $s = 5$, $a = 10$, $A = 2$.
- For improving a given clustering in phase II: $T = 120$ seconds, $s \in \{3 \dots 5\}$, $a \in \{k, \lfloor \frac{k}{2} \rfloor, \lfloor \frac{k}{3} \rfloor\}$ for $k < 20$, and $a \in \{\lfloor \frac{k}{10} \rfloor, \lfloor \frac{k}{20} \rfloor\}$ for larger k 's, $A \in \{3, 4\}$, $e = 3$, $E = +\infty$, $M \in \{2, \dots, 7\}$.

The algorithm is implemented in C and allows fast inference of clusterings with acceptable sizes of separator sets.

B.2 Simulated Annealing

Simulated Annealing (SA), algorithm 3, is applied to the best effort clustering result found with the heuristic two-phase algorithm explained in algorithm 1 and algorithm 2. The heuristic algorithm finds a good k -separator on V upon which SA attempts to improve by $V+$ tiling. By moving voxels around in tiles or newly created tiles the algorithm stages a proposal with the corresponding target t' . This proposal can lead to an improved, no change or worse state. A proposal may be rejected if it leads to a worse state but not necessarily, this to allow exploring other minima in vicinity. The condition $U(0, 1) < f$ with $f : 1/i^{((t'-t)/tp)}$ controls accepting bad proposals, with i the iteration, tp the tuning parameter and $U(0, 1)$ the continuous uniform distribution.

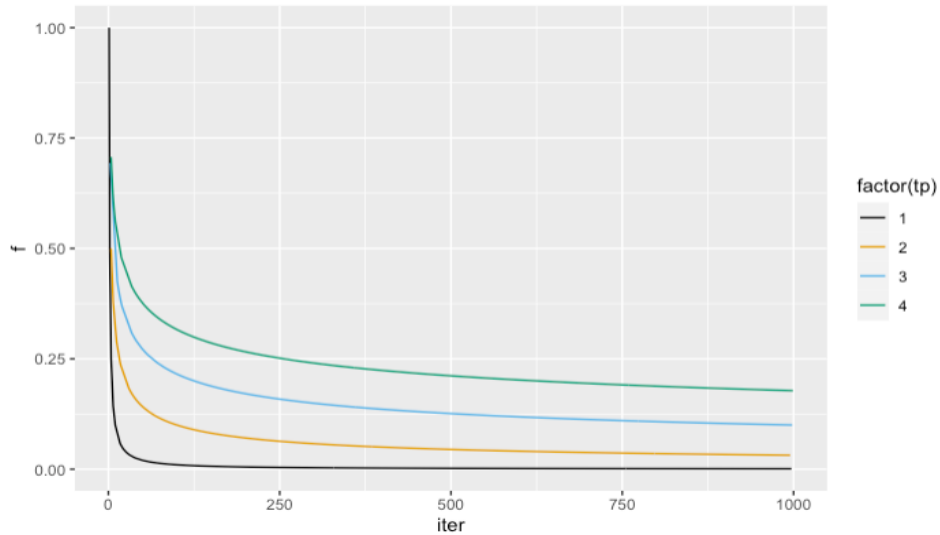


Figure 12: function f with tuning parameter 1 to 4.

Figure.12 shows f when $t' > t$, i.e. a bad proposal. It shows that the probability of accepting a bad proposal diminishes with increasing number of iterations, and it does so more quickly with decreasing tp . The algorithm

terminates when t_{ni} (time no improvement) exceeds $iter$, maximum nr. of iterations allowed.

Algorithm 3: simulated annealing

```

// input parameters;
k ; // size k
tp ; // tuning parameter for acceptance
 $T_1, \dots, T_n$  ; // construct tiles based on the best effort phase-one algorithm
iter ; // max. nr. of iterations
// init;
 $t_{ni} \leftarrow 0$  ; // time no improvement
 $i \leftarrow 0$  ; // total nr. of iterations
 $t \leftarrow t_k(T_1, \dots, T_n)$  ; // target
while True do
     $i++$ ;
     $v \in V^+$  ; // random voxel  $v$ 
     $w \in V^+$  and  $v - w \in \{-1, 0, 1\}^d$  ; //  $w$  is a neighbour of  $v$ 
    //  $T_{\{v\}}$  : tile containing voxel  $v$  ;
    if ( $T_{\{v\}} == T_{\{w\}}$  &  $|T_{\{w\}}^- \cap V| > k$ ) then
        //  $v$  and  $w$  are in the same tile  $T$  and size interior  $T$  is  $> k$  ;
         $t' \leftarrow t_k(T_1, \dots, [v], \dots, T_n)$  ; // add tile  $[v]$  and derive proposed target
    else
         $t' \leftarrow t_k(T_1, \dots, T_{\{w\}} \cup v, \dots, T_n)$  ; // move  $v$  to  $T_{\{w\}}$  and derive proposed target
    // accept/reject proposal? ;
    if  $U(0, 1) < f(i, t, t', tp)$  then
        // accept proposal;
        if  $t' < t$  then
            //  $t'$  is the best so far;
             $t \leftarrow t'$  ; // update target  $t$ 
             $t_{ni} \leftarrow 0$  ; // reset time no improvement
        else
             $t_{ni}++$ ;
    else
        // reject proposal;
         $t_{ni}++$ ;
    if  $t_{ni} \geq iter$  then
        break;

```

C Further pruning illustration

In Figure 13 we illustrate the repeated pruning of the example voxel set V .

D Neurovault analysis

For the Neurovault analysis we downloaded all 543 available collections (April 2019). From these collections we removed all empty collections (16), collections with no valid images (6), collections with no BOLD-fMRI images (127), collections with no statistics images (68), and collections with no group-level statistics images

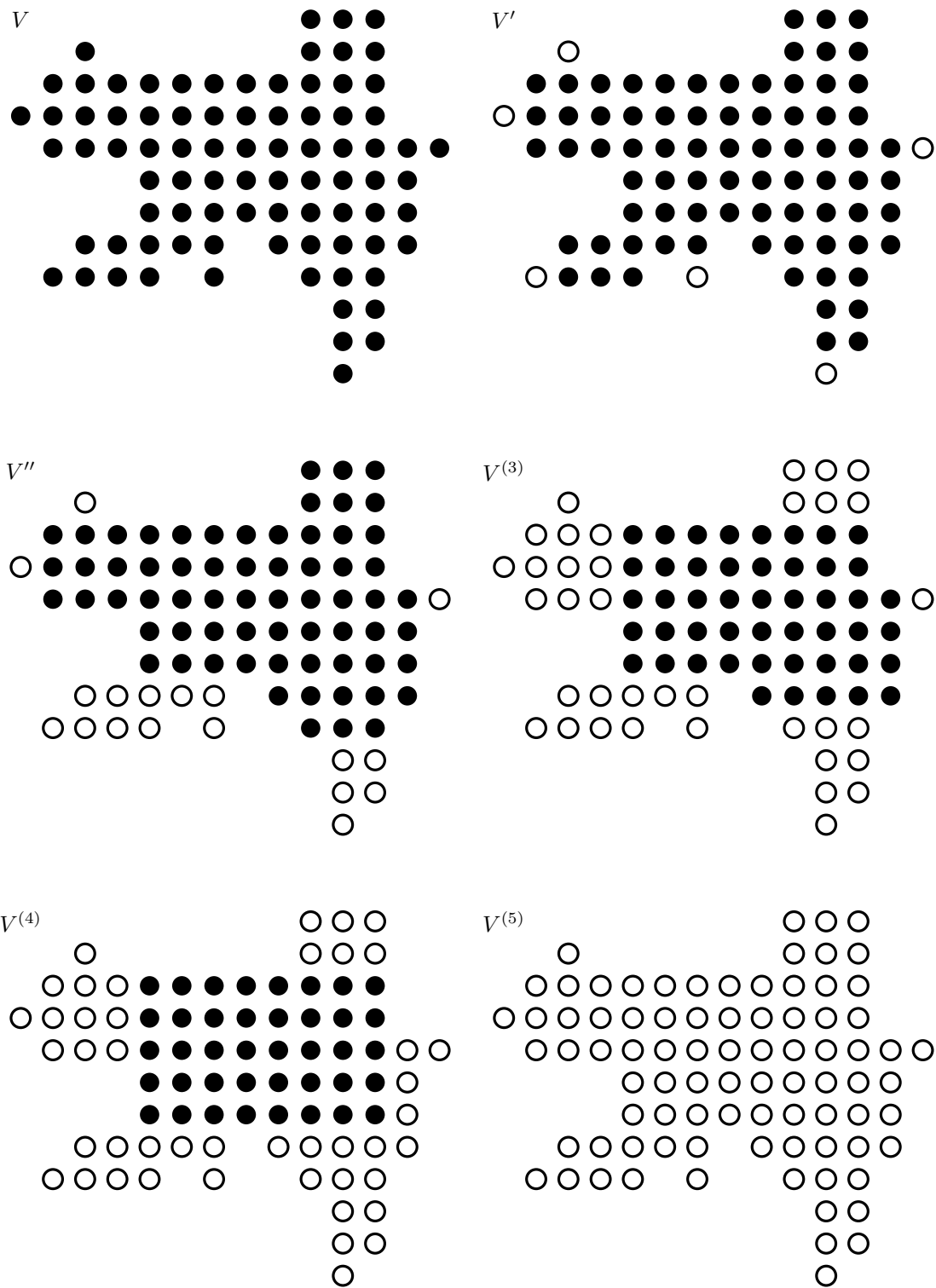


Figure 13: Illustration of the repeated pruning of the voxel set V from Figure 2.

(114). This resulted in 218 valid collections containing 1909 statistics images.

To prevent extreme results we selected a representative sample of images with the following properties: brain size between 10k and 500k voxels, largest cluster size between 1 and 20k voxels, and estimated smoothness smaller than 13 voxels FWHM. This resulted in 1128 valid images for further analysis.

From these images we removed 310 images that were identical or did not contain any clusters with a size larger than the RFT-based cluster size at $\alpha = .05$. The final analyses were thus performed on 818 images.

For each image we performed the following analysis steps:

1. Check type of statistics image
2. If t -value image, check df, when available convert to z -scores, else leave as is.
3. Estimate smoothness on z -statistics image using 'smoothest'
4. Estimate contiguous clusters with $Z > 3.1$
5. Estimate z -threshold value associated with $k_M = 14$
6. Estimate contiguous clusters with z -threshold when $k_M = 14$
7. Calculate cluster-extent p -values based on RFT for all clusters (both for $Z > 3.1$ and $k_M = 14$)
8. Estimate cluster True Discovery Proportion (cTDP) for each cluster (both for $Z > 3.1$ and $k_M = 14$)
9. Calculate voxelwise p -value based on RFT
10. Calculate the number of significant voxels based on voxelwise RFT threshold

E Pseudo code for permutations

Here below we present the pseudo code for finding the z -score threshold with a given cluster extent threshold (see algorithm 4), or computing the cluster extent threshold with a given z -threshold (see algorithm 5), using permutations. The problem of finding supra-threshold clusters for either threshold is equivalent to the standard incremental connectivity problem that can be solved efficiently using a disjoint-set data structure. For each permutation, we find sorted z -scores in $O(m \log m)$ time, and implementing the disjoint-set data structure using the optimized path compression and union by size takes linear time in the size of the output, i.e., $O(v)$ for both algorithms. We suggest using at least 1000 permutations if the total number of permutations is too large.

We note that the permutation z -scores do not need to be pre-calculated; they may be calculated inside the for-loop if storage space is a consideration.

Algorithm 4: Compute the permutation-based z -threshold, corresponding to a given cluster extent threshold, using a disjoint-set data structure.

Input: vectors of size m : $\mathbf{z}_{\pi_1}, \dots, \mathbf{z}_{\pi_N}$ for N permutations (the first permutation is equal to the identity); a pre-specified cluster extent threshold k_M ; a list \mathcal{N} of m vectors, each storing the neighbours of a voxel; a significance level α .

Output: a z -score threshold Z_α .

Function FindZ ($\mathbf{z}_{\pi_1}, \dots, \mathbf{z}_{\pi_N}, k_M, \mathcal{N}, \alpha$)

Initialize a z -score vector \mathbf{Z} for N permutations: $Z[j] = 0$ for $j = 1, \dots, N$.

for $j = 1$ **to** N

Sort \mathbf{z}_{π_j} in descending order such that $z_{\pi_j}[1] \geq \dots \geq z_{\pi_j}[m]$.

Initialize disjoint sets $S_1 = \{1\}, \dots, S_m = \{m\}$.

$v \leftarrow 1$

while $|S_v| \leq k_M$ **do**

$v \leftarrow v + 1$

forall $u \in \mathcal{N}[v]$ such that $u < v$ **do**

 Merge S_v and S_u using union by size and path compression.

$Z[j] \leftarrow z_{\pi_j}[v]$

Sort \mathbf{Z} and find the $(1 - \alpha)$ -quantile $Z_\alpha = Z[\lceil N(1 - \alpha) \rceil]$.

return Z_α

Algorithm 5: Compute the permutation-based cluster extent threshold for a given z -score threshold, using a disjoint-set data structure.

Input: vectors of size m : $\mathbf{z}_{\pi_1}, \dots, \mathbf{z}_{\pi_N}$ for N permutations (the first permutation is equal to the identity); a given z -threshold z ; a list \mathcal{N} of m vectors, each storing the neighbours of a voxel; a significance level α .

Output: a cluster-extent threshold K_α .

Function FindK ($\mathbf{z}_{\pi_1}, \dots, \mathbf{z}_{\pi_N}, z, \mathcal{N}, \alpha$)

Initialize a vector \mathbf{K} for N permutations: $K[j] = 0$ for $j = 1, \dots, N$.

for $j = 1$ **to** N

Sort \mathbf{z}_{π_j} in descending order such that $z_{\pi_j}[1] \geq \dots \geq z_{\pi_j}[m]$.

Initialize disjoint sets $S_1 = \{1\}, \dots, S_m = \{m\}$.

$v \leftarrow 1$

while $z_{\pi_j}[v] > z$ **do**

forall $u \in \mathcal{N}[v]$ such that $u < v$ **do**

 Merge S_v and S_u using union by size and path compression.

$v \leftarrow v + 1$

$K[j] \leftarrow \max\{|S_i| : i < v, i \in \mathbb{Z}^+\}$

Sort \mathbf{K} and find the $(1 - \alpha)$ -quantile $K_\alpha = K[\lceil N(1 - \alpha) \rceil]$.

return K_α

F Application: HCP Working Memory

Based on the new method, TDP bounds were computed for supra-threshold clusters, formed by choosing either cluster-forming threshold or cluster-extent threshold and finding the other threshold based on the conventional Gaussian random field theory (RFT), and the overlapping anatomical regions. Table 4 shows the results for a fixed z -threshold of $z = 3.10$ and $k_M = 32$, and Table 5 shows the results for a given cluster-extent threshold $k_M = 14$ and $z = 3.61$. Consistent with what we observed for permutation inference, the results for RFT also suggest using the cluster-extent threshold $k_M = 14$ instead of the standard z -threshold $z = 3.10$ for better detection power. Similarly, decreasing k_M leads to the increased z and smaller clusters with higher TDP.

References

- Andreella, A., Hemerik, J., Weeda, W., Finos, L., and Goeman, J. (2020). Permutation-based true discovery proportions for fmri cluster analysis. *arXiv preprint arXiv:2012.00368*.
- Barch, D. M., Burgess, G. C., Harms, M. P., Petersen, S. E., Schlaggar, B. L., Corbetta, M., Glasser, M. F., Curtiss, S., Dixit, S., Feldt, C., Nolan, D., Bryant, E., Hartley, T., Footer, O., Bjork, J. M., Poldrack, R., Smith, S., Johansen-Berg, H., Snyder, A. Z., Van Essen, D. C., and Consortium, W.-M. H. (2013). Function in the human connectome: task-fMRI and individual differences in behavior. *NeuroImage*, 15:169–189.
- Beckmann, C. F., Jenkinson, M., and Smith, S. M. (2003). General multilevel linear modeling for group analysis in fmri. *NeuroImage*, 20(2):1052–1063.
- Ben-Ameur, W., Mohamed-Sidi, M.-A., and Neto, J. (2015). The k -separator problem: polyhedra, complexity and approximation results. *Journal of Combinatorial Optimization*, 29(1):276–307.
- Blain, A., Thirion, B., and Neuvial, P. (2022). Notip: Non-parametric true discovery proportion control for brain imaging. *NeuroImage*, page 119492.

Table 4: Results for supra-threshold clusters, defined by the cluster-forming z -threshold $Z > 3.10$ and minimal cluster extent threshold $k_M = 32$ based on RFT.

Cluster				Anatomical region					Position			
ID	size	TDP	LB	Region	size	overlap	TDP	LB	x	y	z	Z_{\max}
1	8870	0.479	0.384	MFG	18250	4049	0.106	0.087	44	72	60	8.87
				FP	33571	2021	0.026	0.020				
				IC	6591	564	0.036	0.028				
2	8526	0.508	0.421	sLOC	27121	5142	0.089	0.071	19	42	61	9.51
				AG	13689	4260	0.150	0.125				
				pSMG	14829	3804	0.125	0.104				
				Precuneous	18119	2491	0.065	0.053				
3	7956	0.444	0.323	Cerebellum	39724	6551	0.075	0.056	63	33	20	9.20
4	6652	0.479	0.383	MFG	18250	4035	0.107	0.087	31	67	64	9.73
				FP	33571	2587	0.035	0.027				
				IC	6591	589	0.037	0.028				
5	350	0.306	0.149	pMTG	11420	310	0.008	0.004	15	46	28	5.18
				tMTG	9735	271	0.008	0.003				
6	100	0.270	0.110	Cerebellum	39724	100	0.001	0.000	49	35	10	6.56
7	59	0.034	0.017	Caudate	4571	51	0.000	0.000	54	68	39	3.92
8	58	0.069	0.017	Cerebellum	39724	58	0.000	0.000	42	36	10	4.85
9	48	0.167	0.021	Thalamus	4602	34	0.000	0.000	43	53	43	4.55
10	45	0.133	0.022	Caudate	4571	45	0.001	0.000	38	67	42	4.38
11	35	0.086	0.029	Cerebellum	39724	35	0.000	0.000	44	41	25	4.20
12	35	0.029	0.029	Thalamus	4602	35	0.000	0.000	42	52	35	5.02
Total	32734	0.472	0.372	MFG	18250	8084	0.213	0.174				
				Cerebellum	39724	6744	0.076	0.056				
				sLOC	27121	5142	0.089	0.071				
				FP	33571	4608	0.061	0.047				
				AG	13689	4260	0.150	0.125				
				pSMG	14829	3804	0.125	0.104				
				Precuneous	18119	2491	0.065	0.053				
				IC	6591	1153	0.073	0.056				
				pMTG	11420	310	0.008	0.004				
				tMTG	9735	271	0.008	0.003				
				Caudate	4571	96	0.002	0.000				
				Thalamus	4602	69	0.001	0.000				

Blanchard, G., Neuvial, P., Roquain, E., et al. (2020). Post hoc confidence bounds on false positives using reference families. *Annals of Statistics*, 48(3):1281–1303.

Bullmore, E., Suckling, J., Overmeyer, S., Rabe-Hesketh, S., Taylor, E., and Brammer, M. (1999). Global, voxel, and cluster tests, by theory and permutation, for a difference between two groups of structural MR images of the brain. *IEEE Transactions on Medical Imaging*, 18(1):32–42.

Chumbley, J., Worsley, K. J., Flandin, G., and Friston, K. J. (2010). Topological FDR for neuroimaging.

- NeuroImage*, 49(4):3057–64.
- Eklund, A., Nichols, T. E., and Knutsson, H. (2016). Cluster failure: Why fMRI inferences for spatial extent have inflated false-positive rates. *Proceedings of the national academy of sciences*, 113(28):7900–7905.
- Forman, S. D., Cohen, J. D., Fitzgerald, M., Eddy, W. F., Mintun, M. A., and Noll, D. C. (1995). Improved Assessment of Significant Activation in Functional Magnetic Resonance Imaging (fMRI): Use of a Cluster-Size Threshold. *Magnetic Resonance in Medicine*, 33(5):636–647.
- Friston, K. J., Frith, C. D., Liddle, P. F., and Frackowiak, R. S. (1991). Comparing functional (PET) images: the assessment of significant change. *Journal of cerebral blood flow and metabolism*, 11(4):690–699.
- Friston, K. J., Worsley, K. J., Frackowiak, R. S., Mazziotta, J. C., and Evans, A. C. (1994). Assessing the significance of focal activations using their spatial extent. *Human brain mapping*, 1(3):210–220.
- Genovese, C. R. and Wasserman, L. (2006). Exceedance control of the false discovery proportion. *Journal of the American Statistical Association*, 101(476):1408–1417.
- Glasser, M. F., Sotiropoulos, S. N., Wilson, J. A., Coalson, T. S., Fischl, B., Andersson, J. L., Xu, J., Jbabdi, S., Webster, M., Polimeni, J. R., Van Essen, D. C., and Jenkinson, M. (2013). The minimal preprocessing pipelines for the Human Connectome Project. *NeuroImage*, 80:105–124.
- Goeman, J. J., Hemerik, J., and Solari, A. (2021). Only closed testing procedures are admissible for controlling false discovery proportions. *The Annals of Statistics*, 49(2):1218–1238.
- Goeman, J. J., Meijer, R. J., Krebs, T. J., and Solari, A. (2019). Simultaneous control of all false discovery proportions in large-scale multiple hypothesis testing. *Biometrika*, 106(4):841–856.
- Goeman, J. J. and Solari, A. (2011). Multiple testing for exploratory research. *Statistical Science*, 26(4):584–597.
- Gorgolewski, K. J., Varoquaux, G., Rivera, G., Schwarz, Y., Ghosh, S. S., Maumet, C., Sochat, V. V., Nichols, T. E., Poldrack, R. A., Poline, J.-B., Yarkoni, T., and Margulies, D. S. (2015). NeuroVault.org: a web-based repository for collecting and sharing unthresholded statistical maps of the human brain. *Frontiers in Neuroinformatics*, 9:8.
- Hayasaka, S. and Nichols, T. E. (2003). Validating cluster size inference: random field and permutation methods. *NeuroImage*, 20(4):2343–2356.
- Jenkinson, M., Beckmann, C. F., Behrens, T. E., Woolrich, M. W., and Smith, S. M. (2012). FSL. *NeuroImage*, 62(2):782–790.
- Lindquist, M. A. (2008). The Statistical Analysis of fMRI Data. *Statistical Science*, 23(4):439–464.
- Marcus, R., Eric, P., and Gabriel, K. R. (1976). On closed testing procedures with special reference to ordered analysis of variance. *Biometrika*, 63(3):655–660.
- Nichols, T. E. (2012). Multiple testing corrections, nonparametric methods, and random field theory. *NeuroImage*, 62(2):811–815.
- Ogawa, S., Tank, D. W., Menon, R., Ellermann, J. M., Kim, S. G., Merkle, H., and Ugurbil, K. (1992). Intrinsic signal changes accompanying sensory stimulation: Functional brain mapping with magnetic resonance imaging. *Proceedings of the National Academy of Sciences of the United States of America*.

- Poline, J. B., Worsley, K. J., Evans, A. C., and Friston, K. J. (1997). Combining Spatial Extent and Peak Intensity to Test for Activations in Functional Imaging. *NeuroImage*, 5(2):83–96.
- Rosenblatt, J. D., Finos, L., Weeda, W. D., Solari, A., and Goeman, J. J. (2018). All-resolutions inference for brain imaging. *Neuroimage*, 181:786–796.
- Van Essen, D. C., Smith, S. M., Barch, D. M., Behrens, T. E. J., Yacoub, E., Ugurbil, K., and Consortium, W.-M. H. (2013). The WU-Minn Human Connectome Project: An overview. *NeuroImage*, 80:62–79.
- Vesely, A., Finos, L., and Goeman, J. J. (2021). Permutation-based true discovery guarantee by sum tests. *arXiv preprint arXiv:2102.11759*.
- Woo, C.-W., Krishnan, A., and Wager, T. D. (2014). Cluster-extent based thresholding in fMRI analyses: Pitfalls and recommendations. *NeuroImage*, 91:412–419.
- Woolrich, M. W., Ripley, B. D., Brady, M., and Smith, S. M. (2001). Temporal autocorrelation in univariate linear modeling of FMRI data. *NeuroImage*, 14(6):1370–1386.
- Worsley, K. J., Evans, A. C., Marrett, S., and Neelin, P. (1992). A Three-Dimensional Statistical Analysis for CBF Activation Studies in Human Brain. *Journal of Cerebral Blood Flow & Metabolism*, 12(6):900–918.
- Worsley, K. J., Marrett, S., Neelin, P., Vandal, A. C., Friston, K. J., and Evans, A. C. (1996). A unified statistical approach for determining significant signals in images of cerebral activation. *Human Brain Mapping*, 4(1):58–73.
- Yannakakis, M. (1981). Node-deletion problems on bipartite graphs. *SIAM Journal on Computing*, 10(2):310–327.

Table 5: Results for supra-threshold clusters, defined by the cluster-forming z -threshold of $Z > 3.61$, based on RFT, and minimal cluster extent threshold $k_M = 14$.

Cluster				Anatomical region					Position			
ID	size	TDP	LB	Region	size	overlap	TDP	LB	x	y	z	Z_{\max}
1	7415	0.607	0.534	sLOC	27121	4419	0.094	0.080	19	42	61	9.51
				AG	13689	3846	0.166	0.147				
				pSMG	14829	3426	0.137	0.122				
				Precuneous	18119	2182	0.069	0.060				
2	7158	0.580	0.493	MFG	18250	3336	0.106	0.091	44	72	60	8.87
				SFG	18946	2976	0.089	0.075				
				poIFG	8301	1410	0.092	0.077				
				IC	6591	500	0.041	0.034				
3	5655	0.550	0.440	Cerebellum	39724	5081	0.071	0.058	63	33	20	9.20
4	5347	0.578	0.492	MFG	18250	3405	0.109	0.094	31	67	64	9.73
				FP	33571	1960	0.032	0.027				
				IC	6591	526	0.042	0.036				
5	223	0.413	0.202	OP	15486	173	0.004	0.002	39	22	36	5.72
				ICC	7134	121	0.007	0.004				
6	151	0.384	0.205	pMTG	11420	151	0.005	0.003	15	46	28	5.18
7	69	0.377	0.188	Cerebellum	39724	69	0.001	0.000	49	35	10	6.56
8	69	0.377	0.130	FP	33571	69	0.001	0.000	31	86	29	5.77
9	61	0.344	0.164	FP	33571	61	0.001	0.000	57	88	29	5.16
10	44	0.341	0.136	OP	15486	44	0.001	0.000	51	15	42	5.35
11	27	0.222	0.037	Thalamus	4602	21	0.001	0.000	43	53	43	4.55
12	23	0.087	0.043	Cerebellum	39724	23	0.000	0.000	42	36	10	4.85
13	20	0.250	0.050	Caudate	4571	20	0.001	0.000	38	67	42	4.38
14	19	0.053	0.053	Cerebellum	39724	19	0.000	0.000	42	32	28	4.19
15	17	0.176	0.059	tMTG	9735	17	0.000	0.000	18	41	32	4.13
16	16	0.125	0.063	Thalamus	4602	16	0.000	0.000	42	52	35	5.02
Total	26314	0.574	0.484	MFG	18250	6741	0.215	0.185				
				Cerebellum	39724	5192	0.072	0.058				
				sLOC	27121	4419	0.094	0.080				
				AG	13689	3846	0.166	0.147				
				pSMG	14829	3426	0.137	0.122				
				SFG	18946	2976	0.089	0.075				
				Precuneous	18119	2182	0.069	0.060				
				FP	33571	2090	0.034	0.027				
				poIFG	8301	1410	0.092	0.077				
				IC	6591	1026	0.083	0.070				
				OP	15486	217	0.005	0.002				
				pMTG	11420	151	0.005	0.003				
				ICC	7134	121	0.007	0.004				
				Thalamus	4602	37	0.001	0.000				
				Caudate	4571	20	0.001	0.000				
				tMTG	9735	17	0.000	0.000				